



Ordovician Proto-basin in South China and its Tectonic Implications: Evidence from the Detrital Zircon U-Pb Ages of the Ordovician in Central Hunan, China

ZHANG Jibiao¹, NI Jingbo², LIU Yanxue^{1,*}, ZHANG Heng¹ and BU Ling³

¹ Institute of Geology, Chinese Academy of Geological Sciences, Beijing 100037, China

² Beijing Institute of Geological Survey, Beijing 102206, China

³ Hebei Regional Geological Survey Institute, Hebei 050081, China

Abstract: Caledonian orogeny is another important tectonic event in South China Block after the breakup of the Rodinia supercontinent. With a view to constrain the tectonic evolution and proto-basin in South China, this paper reports the geochemical and zircon U-Pb dating data of the Ordovician strata in central Hunan, South China. Geochemical features and paleocurrent directions suggest that the lower Ordovician deposited in a passive continental margin basin with a provenance of quartzose components and showing an affinity with the Yangtze Block. U-Pb age data for 260 detrital zircons from upper Ordovician identify three major age populations as: 900–1200 Ma, 1400–1800 Ma and 2400–2700 Ma. The detrital zircon age spectrum as well as the paleocurrent directions suggest that upper Ordovician deposited in a foreland basin and showing a close affinity with the Cathaysia Block. It is also suggest that the lower Ordovician continuously accepted the mineral from the Yangtze Block, whereas the provenance of the upper Ordovician sedimentary basin changed from the Yangtze Block to the Cathaysia Block. This change implies a tectonic movement, which caused the transformation of the proto-basin in the Hunan area in SCB from passive continental margin basin to foreland basin probably took place during late Ordovician. This fact also demonstrate that the Caledonian orogeny in South China Block began no later than 453 Ma, and a new crustal evolution model is proposed.

Key words: U-Pb chronology, Ordovician, Proto-basin, Caledonian orogeny, South China

Citation: Zhang et al., 2020. Ordovician Proto-basin in South China and its Tectonic Implications: Evidence from the Detrital Zircon U-Pb Ages of the Ordovician in Central Hunan, China. *Acta Geologica Sinica (English Edition)*, 94(6): 2115–2133. DOI: 10.1111/1755-6724.14583

1 Introduction

The South China Block (SCB), composed of the Yangtze Block to the northwest and the Cathaysia Block to the southeast (Fig. 1). It is widely accepted that the two blocks were amalgamated during the Neoproterozoic along the Shaoxing–Jiangshan–Pingxiang fault zone and formed the Jiangnan orogen (also known as the Sibao orogen) (Zhao and Cawood, 1999; Zhou et al., 2009; Li et al., 2007, 2010b; Wang et al., 2012; Zhao et al., 2015; Yao et al., 2015, 2016; Chen et al., 2018; Guo et al., 2018; Jiang et al., 2018; Zhao et al., 2018). After the end of Neoproterozoic orogeny, the SCB underwent multiple tectonic movements during the early Paleozoic under the influence of Caledonian orogeny which is marked by a regional unconformity between pre-Devonian and Devonian strata (BGMRHN, 1988; Ting, 1929; Shu, 2006; Li et al., 2010; Wang et al., 2010b). Caledonian movement can provide important information about the tectonic evolution processes of the SCB. They have thus received more attention in the last few decades (Ren, 1991; Xu et al., 2001; Shu, 2006; Chen et al., 2000, 2006, 2010; Li et al., 2010; Wang et al., 2011; Pang et al., 2011; He et al.,

2016;). However, interpretation of geochemical data and geodynamics are not unequivocal, which has led to contrasting views on the proto-basin as well as the tectonic implications in SCB (Yuan et al., 1997; Wang et al., 2011; Luo et al., 2012; Xu et al., 2012; Yao et al., 2015). Some researchers believe that the SCB was always a rift basin in the early Paleozoic (Wang et al., 2001; Yang et al., 2012). Other workers consider that the southeastern margin of the Yangtze Block evolving from a passive continental margin basin environment in the early Paleozoic, to a foreland basin setting in the late Ordovician to Silurian (Bai et al., 2007; Yin et al., 2001; Chen et al., 2012; Xu et al., 2012; Yao et al., 2015). The study area in central Hunan Province is located at the boundary of the Yangtze and Cathaysia blocks and is the key area for studying basic geology of the SCB (Fig. 1). Thus, systematic studies on the Ordovician strata of the Hunan area will provide a better understanding on the nature and tectonic evolution process of the SCB.

In this paper, we carry out systematic field investigations in the Hunan province, focus on the Jingtou–Jinlan and Shuangfeng–Qiaotingzi stratigraphic cross-section, and sample the sediments from Baishuixi Formation, Qiaotingzi Formation and Tianmashan Formation. Thirty-seven sedimentary samples were

* Corresponding author. E-mail: lyanxue@soho.com

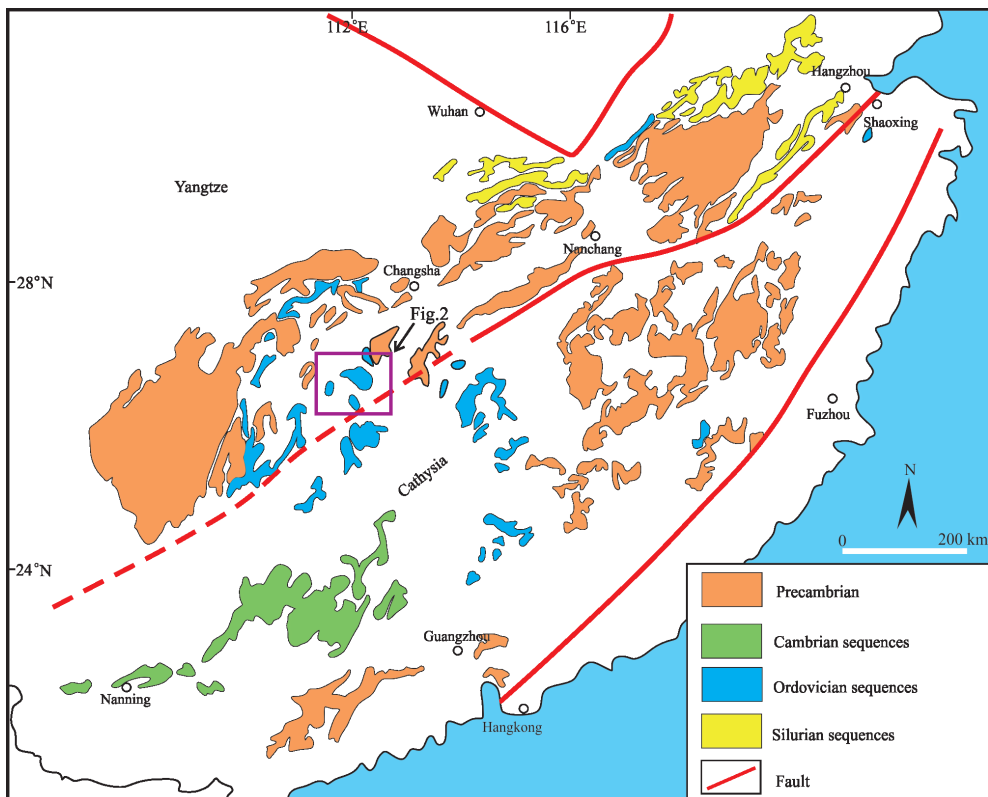


Fig. 1. Geological map showing the distribution of early Paleozoic rocks in the South China Block.

collected for comprehensive detrital zircon U-Pb and geochemistry analyses. In conjunction with previous data, we propose a new basin evolution model in the South China Block during the Ordovician.

2 Geological Settings

The South China Block comprise the Yangtze Block to the northwest and the Cathaysia Block to the southeast, bounded by the Jiangnan orogen between them (Fig. 1). The oldest rocks of the Yangtze Block, represented by the Kongling Group to the north and yielded ages ranging from 3.2 to 1.8 Ga (Gao et al., 1999; Qiu et al., 2000; Zheng et al., 2006). Late Paleoproterozoic to Mesoproterozoic strata to the west, including the Huili, Kunyang and Dongchuan Groups, tuff and igneous rocks (both intrusive and volcanic) in these sequences constrain the depositional ages of these strata at 1.7–1.0 Ga (Greentree and Li, 2008; Zhao et al., 2010; Geng et al., 2017). Early Neoproterozoic rocks, such as the Shuangxiwu, Shuangqiaoshan and Heshangzhen Groups are widespread in the southeastern Yangtze Block, have yield ages in the range 960–760 Ma (Wang et al., 2007; Yao et al., 2014; Li et al., 2009). Numerous Early–Middle Neoproterozoic igneous rock mostly distributed around the margin of the Yangtze Block (Zhou et al., 2002; Li et al., 2003; Zheng et al., 2007, 2008; Li et al., 2009; Wang et al., 2010a). Precambrian strata in the Cathaysia Block mainly distributed in the Wuyi–Yukai Domains, yield mainly Proterozoic ages (Li et al., 2002; Wan et al., 2007; Xiang et al., 2008; Yu et al., 2009, 2010; Li et al., 2011a).

The oldest rocks exposed in the Hunan Province are the Neoproterozoic strata, and contain the Sizhoushan, Tianzidi, and Liucapo Formations to the south and Gaojian Group to the west. The Sizhoushan Formation consists of gray slate and sandy slate. The Tianzidi Formation consists of siliceous rocks and grey–green lithic sandstones. The Liuchapo Formation contains only siliceous rocks. The Gaojian Group consists mainly of sandstones, calcareous slates, marbles, and tuffaceous slates. The Cambrian strata include the Xiangnan, Chayuantou, and Xiaozijin Formations to the south and the Tashan Group to the west. The Cambrian strata to the south consists mainly of low-grade metasandstones with less pelitic slates, slates rocks, fine-grained quartz sandstones and carbonaceous slates (BGMRHN, 1988).

3 Stratigraphic Section and Samples

This study is focused on the Ordovician strata on the southeastern margin of the Yangtze Block. The Ordovician strata can been divided into four formations from bottom to top termed as the lower Ordovician Baishuixi and Qiaotingzi Formations, the middle Ordovician Yanxi Formation and the upper Ordovician Tianmashan Formation (Fig. 4). The Baishuixi Formation is conformably underlain by the upper Cambrian Tanxi Formation. It consists mainly of gray mudstone and siltstone, interstratified with thin fine-grained sandstone and sericite slate. It contains the Ordovician *Didymograptus hirundo* sp. and *Palaeobolus* sp. (BGMRHN, 1988). The Qiaotingzi Formation comprises

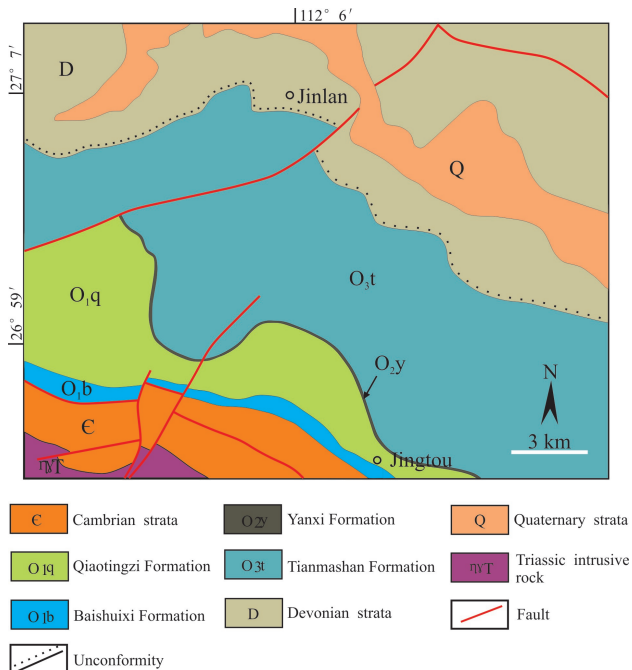


Fig. 2. Distribution of the Ordovician stratigraphy, Hunan province, South China (modified after BGMRHN, 1988).

silty slate and sericite-chlorite slate. It contains the Ordovician *Obolus* sp. (BGMRHN, 1988). The Yanxi Formation composed of a succession of black carbonaceous siliceous shale, siliceous rock and carbonaceous slate. The shale has thinly laminated bedding and deep water sedimentary structures such as horizontal bedding. It contains the *Tetragraptus* sp. and *Climacograptus truncatus* sp. (BGMRHN, 1988). The Tianmashan Formation is composed mainly of the gray

fine grained sandstone, quartz sandstone and siltstone, interstratified with carbonaceous shale. Evidence for deposition in a deep water slope environment includes bouma sequence, cross bedding and horizontal bedding. This Formation is unconformably covered by lower Silurian sequences.

Based on detailed field investigation, three fine sandstone samples were collected from the Tianmashan Formation for U-Pb dating and Thirty-four sedimentary rocks samples were collected from the Baishuixi and Qiaotingzi Formations for geochemical analysis in order to constrain the depositional ages, provenance and tectonic setting.

4 Analytical Methods

4.1 U-Pb zircon analyses

LA-ICP-MS analyses of zircon U-Pb isotopic compositions were performed using an Neptune MC-ICP-MS attached to a NEW Wave 213 nm laser ablation system at the Key laboratory of mineralization and resource evaluation, Chinese academy of geological sciences (CAGS). The instrument has a laser spot diameter of 25 μm , an operating voltage of 27.1 KV, a gas flow rate of 270 ml/min, and a laser energy of 29 J/cm². A blank signal of approximately 15 seconds and a sample signal of 45 seconds constitute the data signal of the sample. U-Pb isotope dating was performed using zircon standard GJ-1 as an external standard for isotope fractionation correction (Liu et al., 2010). For each 10 sample points analyzed, GJ-1 was analyzed twice. The final U-Pb age harmonic map of zircon samples using Isoplot/Exver3 (Ludwig, 2003).

4.2 Geochemistry

Whole-rock major element analyses were performed



Fig. 3. Representative field photos of major rock types in this study.

(a) Baishuixi Formation gray siltitesandstone with horizontal bedding; (b) Qiaotingzi Formation fine-sandstone with oblique bedding; (c) Tianmashan Formation turbidite with bouma sequence; (d) photo-micrograph of Tianmashan Formation coarse sample with oblique bedding.

Table 1 U-Pb data for zircons in sandstone from the Tianmashan Formation in South China

20161026-2	Elemental abundance (ppm)			$^{207}\text{Pb}/^{206}\text{Pb}$		$^{207}\text{Pb}/^{235}\text{U}$		$^{206}\text{Pb}/^{238}\text{U}$		$^{207}\text{Pb}/^{206}\text{Pb}$		$^{207}\text{Pb}/^{235}\text{U}$		$^{206}\text{Pb}/^{238}\text{U}$		Concordance	
	Pb	Th	U	Th/U	Ratio	1 σ	Ratio	1 σ	Ratio	1 σ	Age (Ma)	10	15	2252	32		
1026-2-1	427	721	708	1.02	0.1584	0.0014	9.1638	0.1549	0.4182	0.0071	2438	10	2355	15	2252	32	95%
1026-2-2	118	237	329	0.72	0.1039	0.0011	3.9598	0.0775	0.2753	0.0050	1695	19	1626	16	1568	25	96%
1026-2-3	66	284	330	0.86	0.0728	0.0010	1.5172	0.0307	0.1510	0.0032	1009	25	937	12	907	18	96%
1026-2-4	49	187	208	0.90	0.0775	0.0012	1.8945	0.0843	0.1765	0.0058	1144	31	1079	30	1048	32	97%
1026-2-5	141	192	270	0.71	0.1564	0.0016	8.3867	0.1147	0.3883	0.0055	2417	182	2274	12	2115	25	92%
1026-2-6	493	368	778	0.47	0.2018	0.0018	13.5441	0.2037	0.4853	0.0069	2843	14	2718	14	2550	30	93%
1026-2-7	74	296	381	0.78	0.0735	0.0009	1.5483	0.0312	0.1525	0.0028	1028	24	950	12	915	16	96%
1026-2-8	72	133	306	0.44	0.0860	0.0018	2.3987	0.0583	0.2022	0.0049	1339	39	1242	17	1187	26	95%
1026-2-9	126	186	377	0.49	0.0991	0.0010	3.8302	0.0667	0.2797	0.0045	1607	17	1599	14	1590	23	99%
1026-2-10	431	305	1490	0.20	0.1008	0.0010	3.8786	0.1317	0.2785	0.0093	1639	19	1609	27	1584	47	98%
1026-2-11	80	53	185	0.29	0.1251	0.0013	6.4088	0.1485	0.3712	0.0084	2031	20	2033	20	2035	39	99%
1026-2-12	104	129	261	0.49	0.1135	0.0014	5.0931	0.0804	0.3257	0.0060	1857	22	1835	13	1818	29	99%
1026-2-13	167	132	865	0.15	0.0752	0.0010	1.8734	0.0497	0.1810	0.0050	1076	26	1072	18	1072	27	99%
1026-2-14	375	1169	1140	1.03	0.0930	0.0008	3.0693	0.0684	0.2389	0.0053	1489	17	1425	17	1381	27	96%
1026-2-15	160	99	222	0.45	0.2743	0.0027	20.1016	0.7002	0.5285	0.0164	3331	16	3096	34	2735	69	87%
1026-2-16	64	144	529	0.27	0.0637	0.0009	0.9428	0.0281	0.1066	0.0023	731	29	674	15	653	13	96%
1026-2-17	207	596	526	1.13	0.1067	0.0010	4.5212	0.0753	0.3072	0.0051	1743	18	1735	14	1727	25	99%
1026-2-18	101	47	857	0.05	0.0625	0.0007	0.9431	0.0222	0.1093	0.0025	700	9	675	12	669	14	99%
1026-2-19	54	222	262	0.84	0.0718	0.0008	1.5509	0.0338	0.1562	0.0029	989	18	951	13	936	16	98%
1026-2-20	60	297	192	1.55	0.0862	0.0014	2.4552	0.0451	0.2063	0.0025	1343	32	1259	13	1209	13	95%
1026-2-21	451	649	574	1.13	0.1978	0.0018	14.6732	0.3226	0.5370	0.0110	2809	19	2794	21	2771	46	99%
1026-2-22	69	139	96	1.46	0.1656	0.0015	10.6835	0.1834	0.4674	0.0074	2513	15	2496	16	2472	33	99%
1026-2-23	68	170	431	0.39	0.0686	0.0008	1.4544	0.0507	0.1521	0.0046	887	22	912	21	913	26	99%
1026-2-24	127	311	1008	0.31	0.0655	0.0011	0.9895	0.0254	0.1091	0.0019	791	33	698	13	667	11	95%
1026-2-25	85	74	430	0.17	0.0774	0.0012	1.8716	0.0488	0.1751	0.0033	1131	32	1071	17	1040	18	97%
1026-2-26	74	125	361	0.35	0.0751	0.0007	1.8176	0.0292	0.1755	0.0025	1070	17	1052	11	1042	14	99%
1026-2-27	148	1500	880	1.70	0.0638	0.0007	0.9792	0.0286	0.1116	0.0035	744	22	693	15	682	20	98%
1026-2-28	248	206	633	0.33	0.1131	0.0010	5.1115	0.0877	0.3273	0.0050	1850	15	1838	15	1825	24	99%
1026-2-29	86	375	242	1.55	0.0912	0.0011	3.0012	0.0816	0.2387	0.0061	1450	22	1408	21	1380	32	98%
1026-2-30	558	522	2562	0.20	0.0807	0.0008	2.2969	0.0417	0.2070	0.0041	1215	20	1211	13	1213	22	99%
1026-2-31	1822	849	4594	0.18	0.1596	0.0012	7.2462	0.1208	0.3290	0.0055	2451	13	2142	15	1834	27	84%
1026-2-32	62	493	319	1.54	0.0686	0.0018	1.2349	0.0454	0.1307	0.0041	887	54	817	21	792	23	96%
1026-2-33	143	144	282	0.51	0.1386	0.0012	7.6398	0.1297	0.4003	0.0071	2210	15	2190	15	2170	33	99%
1026-2-34	366	175	453	0.39	0.3072	0.0026	24.5594	0.3536	0.5802	0.0089	3507	13	3291	14	2950	36	89%
1026-2-35	409	329	758	0.43	0.1551	0.0019	9.4894	0.1691	0.4455	0.0090	2403	25	2387	16	2375	40	99%
1026-2-36	137	189	290	0.65	0.1558	0.0014	7.6507	0.1141	0.3564	0.0057	2411	15	2191	13	1965	27	89%
1026-2-37	346	470	1434	0.33	0.0811	0.0009	2.3359	0.0441	0.2092	0.0045	1233	11	1223	13	1225	24	99%
1026-2-38	265	253	393	0.64	0.1870	0.0016	13.2495	0.2214	0.5138	0.0084	2716	15	2698	16	2673	36	99%
1026-2-39	40	305	381	0.80	0.0582	0.0009	0.6771	0.0148	0.0845	0.0017	539	35	525	9	523	10	99%
1026-2-40	87	92	360	0.26	0.0810	0.0013	2.3766	0.0629	0.2122	0.0041	1222	31	1236	19	1240	22	99%
1026-2-41	203	550	781	0.70	0.0830	0.0009	2.3795	0.0479	0.2079	0.0040	1269	26	1236	14	1218	21	98%
1026-2-42	142	369	545	0.68	0.0849	0.0009	2.4377	0.0574	0.2080	0.0048	1314	53	1254	17	1218	26	97%
1026-2-43	87	328	314	1.04	0.0802	0.0011	2.2878	0.0442	0.2068	0.0036	1203	26	1209	14	1212	19	99%
1026-2-44	84	86	171	0.50	0.1362	0.0012	7.4984	0.1448	0.3994	0.0077	2189	16	2173	17	2166	35	99%
1026-2-45	52	153	277	0.55	0.0713	0.0008	1.5056	0.0305	0.1530	0.0029	969	23	933	12	918	16	98%
1026-2-46	71	218	376	0.58	0.0710	0.0007	1.4946	0.0292	0.1526	0.0028	967	11	928	12	916	16	98%
1026-2-47	230	318	847	0.38	0.1133	0.0013	3.4155	0.0820	0.2183	0.0047	1854	22	1508	19	1273	25	83%
1026-2-48	196	1063	628	1.69	0.0804	0.0010	2.3023	0.0570	0.2079	0.0051	1207	24	1213	18	1217	27	99%
1026-2-49	185	327	746	0.44	0.0904	0.0010	2.5128	0.0907	0.2012	0.0058	1435	21	1276	26	1182	31	92%
1026-2-50	146	280	827	0.34	0.0727	0.0011	1.5420	0.0495	0.1530	0.0040	1006	30	947	20	918	23	96%
1026-2-51	312	181	304	0.59	0.3213	0.0028	31.3786	0.6430	0.7091	0.0157	3576	13	3531	20	3455	59	97%
1026-2-52	120	340	376	0.90	0.0923	0.0010	3.0615	0.0619	0.2405	0.0046	1473	20	1423	15	1389	24	97%
1026-2-53	207	310	845	0.37	0.0825	0.0008	2.3790	0.0416	0.2093	0.0039	1258	18	1236	13	1225	21	99%
1026-2-54	41	231	244	0.95	0.0702	0.0015	1.2392	0.0297	0.1281	0.0022	1000	38	819	13	777	13	94%
1026-2-55	422	482	940	0.51	0.1573	0.0015	7.5668	0.1363	0.3491	0.0069	2428	16	2181	16	1930	33	87%
1026-2-56	59	169	274	0.62	0.0754	0.0009	1.8415	0.0360	0.1770	0.0033	1081	24	1060	13	1051	18	99%
1026-2-57	53	202	187	1.08	0.0850	0.0011	2.4260	0.0486	0.2073	0.0044	1317	20	1250	14	1214	23	97%
1026-2-58	92	207	503	0.41	0.0724	0.0008	1.5414	0.0326	0.1545	0.0033	998	24	947	13	926	19	97%
1026-2-59	37	114	332	0.34	0.0629</												

Continued Table 1

20161026-2	Elemental abundance (ppm)			$^{207}\text{Pb}/^{206}\text{Pb}$		$^{207}\text{Pb}/^{235}\text{U}$		$^{206}\text{Pb}/^{238}\text{U}$		$^{207}\text{Pb}/^{206}\text{Pb}$		$^{207}\text{Pb}/^{235}\text{U}$		$^{206}\text{Pb}/^{238}\text{U}$		Concordance	
	Pb	Th	U	Ratio	1 σ	Ratio	1 σ	Ratio	1 σ	Age (Ma)	1 σ	2 σ	1 σ	2 σ			
1026-2-70	278	249	545	0.46	0.1585	0.0007	8.6814	0.1602	0.3956	0.0071	2440	9	2305	17	2149	33	92%
1026-2-71	354	81	994	0.08	0.1157	0.0007	5.2144	0.1152	0.3259	0.0071	1891	11	1855	19	1818	35	98%
1026-2-72	175	141	880	0.16	0.0735	0.0009	1.8225	0.0423	0.1790	0.0031	1028	23	1054	15	1061	17	99%
1026-2-73	52	294	196	1.50	0.0769	0.0008	1.8878	0.0302	0.1775	0.0022	1120	21	1077	11	1053	12	97%
1026-2-75	306	493	739	0.67	0.1380	0.0014	6.0722	0.1828	0.3183	0.0088	2202	18	1986	26	1781	43	89%
1026-2-76	110	470	559	0.84	0.0686	0.0012	1.4291	0.0478	0.1508	0.0043	887	37	901	20	905	24	99%
1026-2-77	45	118	97	1.22	0.1131	0.0016	5.0530	0.1079	0.3237	0.0059	1850	21	1828	18	1808	29	98%
1026-2-78	470	392	883	0.44	0.1786	0.0016	10.9498	0.2728	0.4440	0.0106	2640	15	2519	23	2369	47	93%
1026-2-79	107	169	526	0.32	0.0766	0.0009	1.8695	0.0337	0.1772	0.0032	1122	28	1070	12	1051	18	98%
1026-2-80	218	266	342	0.78	0.1822	0.0017	11.9565	0.2513	0.4757	0.0095	2673	15	2601	20	2509	41	96%
1026-2-81	43	130	286	0.45	0.0668	0.0009	1.1882	0.0322	0.1290	0.0031	831	169	795	15	782	18	98%
1026-2-82	85	276	362	0.76	0.0768	0.0010	1.8712	0.0416	0.1772	0.0042	1117	21	1071	15	1052	23	98%
1026-2-83	60	142	481	0.29	0.0650	0.0008	0.9698	0.0189	0.1084	0.0020	772	27	688	10	663	12	96%
1026-2-84	64	80	454	0.18	0.0663	0.0009	1.1652	0.0220	0.1275	0.0019	817	34	784	10	773	11	98%
1026-2-85	151	586	807	0.73	0.0723	0.0006	1.5002	0.0255	0.1506	0.0026	994	12	930	10	904	14	97%
20161027-2																	
1027-2-1	258	182	592	0.31	0.1627	0.0014	9.9618	0.1274	0.4439	0.0053	2484	15	2431	12	2368	23	97%
1027-2-2	502	156	1371	0.11	0.1601	0.0017	8.4348	0.0998	0.3819	0.0038	2457	19	2279	11	2085	18	91%
1027-2-3	187	515	683	0.75	0.0923	0.0011	3.1355	0.0381	0.2460	0.0024	1474	24	1441	9	1418	12	98%
1027-2-4	65	130	125	1.04	0.1622	0.0017	9.3697	0.1510	0.4181	0.0055	2480	19	2375	15	2252	25	94%
1027-2-5	107	570	591	0.96	0.0678	0.0008	1.4094	0.0272	0.1502	0.0020	861	22	893	11	902	11	98%
1027-2-6	80	108	420	0.26	0.0746	0.0008	1.8521	0.0311	0.1799	0.0031	1057	20	1064	11	1066	17	99%
1027-2-7	46	219	225	0.97	0.0741	0.0011	1.6317	0.0367	0.1592	0.0030	1044	29	983	14	952	17	96%
1027-2-8	25	69	229	0.30	0.0602	0.0012	0.7886	0.0228	0.0946	0.0021	609	41	590	13	583	13	98%
1027-2-9	68	187	297	0.63	0.0761	0.0009	1.9015	0.0355	0.1805	0.0030	1098	24	1082	12	1070	16	98%
1027-2-10	47	128	356	0.36	0.0630	0.0009	0.9424	0.0205	0.1081	0.0021	707	34	674	11	661	12	98%
1027-2-11	185	426	681	0.63	0.0836	0.0010	2.3981	0.0389	0.2074	0.0033	1283	24	1242	12	1215	18	97%
1027-2-12	124	224	695	0.32	0.0722	0.0008	1.4728	0.0285	0.1472	0.0025	994	21	919	12	885	14	96%
1027-2-13	163	933	654	1.43	0.0713	0.0007	1.5870	0.0323	0.1606	0.0030	969	20	965	13	960	17	99%
1027-2-14	89	137	471	0.29	0.0722	0.0008	1.5887	0.0313	0.1596	0.0034	991	21	966	12	955	19	98%
1027-2-15	98	75	116	0.64	0.2289	0.0020	18.9910	0.3494	0.6006	0.0118	3044	13	3041	18	3032	47	99%
1027-2-16	17	293	108	2.71	0.1275	0.0043	1.6482	0.0705	0.0927	0.0015	2065	59	989	27	571	9	46%
1027-2-17	218	625	1099	0.57	0.0727	0.0007	1.6105	0.0359	0.1602	0.0035	1006	19	974	14	958	20	98%
1027-2-18	476	36	839	0.04	0.1671	0.0018	10.9573	0.1954	0.4745	0.0085	2529	12	2520	17	2503	37	99%
1027-2-19	48	140	237	0.59	0.0714	0.0009	1.5732	0.0290	0.1597	0.0028	969	26	960	11	955	16	99%
1027-2-20	45	94	175	0.54	0.0812	0.0011	2.3258	0.0450	0.2076	0.0036	1228	27	1220	14	1216	19	99%
1027-2-21	68	364	360	1.01	0.0703	0.0009	1.4400	0.0429	0.1482	0.0042	939	21	906	18	891	24	98%
1027-2-22	42	449	297	1.51	0.0594	0.0069	0.7706	0.0471	0.0945	0.0054	589	256	580	27	582	32	99%
1027-2-23	141	446	376	1.19	0.0946	0.0011	3.4751	0.0633	0.2657	0.0038	1521	23	1522	14	1519	20	99%
1027-2-24	81	259	438	0.59	0.0705	0.0009	1.4489	0.0392	0.1492	0.0040	944	24	909	16	897	22	98%
1027-2-25	96	162	389	0.42	0.0809	0.0008	2.3187	0.0411	0.2075	0.0034	1220	14	1218	13	1216	18	99%
1027-2-26	80	170	383	0.44	0.0770	0.0008	1.9132	0.0473	0.1800	0.0042	1121	20	1086	17	1067	23	98%
1027-2-27	96	112	208	0.54	0.1276	0.0012	6.4681	0.1293	0.3675	0.0072	2066	17	2042	18	2018	34	98%
1027-2-28	195	561	462	1.22	0.1056	0.0010	4.5198	0.1165	0.3109	0.0082	1725	17	1735	21	1745	40	99%
1027-2-29	157	295	1530	0.19	0.0581	0.0005	0.7570	0.0128	0.0945	0.0014	532	16	572	7	582	8	98%
1027-2-30	210	101	1336	0.08	0.0687	0.0007	1.4117	0.0289	0.1492	0.0029	889	16	894	12	896	16	99%
1027-2-31	25	130	150	0.87	0.0685	0.0019	1.2314	0.0429	0.1303	0.0031	883	55	815	20	790	18	96%
1027-2-32	117	194	654	0.30	0.0717	0.0008	1.5747	0.0371	0.1593	0.0034	977	29	960	15	953	19	99%
1027-2-33	170	278	557	0.50	0.1134	0.0013	4.0071	0.0558	0.2564	0.0042	1854	19	1636	11	1471	22	89%
1027-2-34	100	217	543	0.40	0.0711	0.0007	1.5682	0.0330	0.1598	0.0030	961	20	958	13	955	17	99%
1027-2-35	48	39	488	0.08	0.0585	0.0007	0.7537	0.0151	0.0934	0.0017	546	24	570	9	576	10	99%
1027-2-36	84	278	425	0.65	0.0712	0.0007	1.5726	0.0267	0.1604	0.0027	963	20	959	11	959	15	99%
1027-2-37	413	1270	1161	1.09	0.0945	0.0008	3.4755	0.0818	0.2658	0.0055	1520	21	1522	19	1519	28	99%
1027-2-38	164	61	1041	0.06	0.0688	0.0007	1.4062	0.0281	0.1483	0.0029	900	25	892	12	892	16	99%
1027-2-39	102	522	484	1.08	0.0743	0.0009	1.6044	0.0269	0.1563	0.0018	1050	25	972	10	936	10	96%
1027-2-40	231	461	568	0.81	0.1102	0.0010	4.6953	0.0768	0.3088	0.0048	1803	17	1766	14	1735	24	98%
1027-2-41	224	162	1394	0.12	0.0676	0.0006	1.3803	0.0169	0.1479	0.0016	857	19	881	7	889	9	99%
1027-2-42	210	698	1144	0.61	0.0698	0.0006	1.4164	0.0270	0.1471	0.0027	924	17	896	11	885	15	98%
1027-2-43	139	406	437	0.93</													

Continued Table 1

20161027-2	Elemental abundance (ppm)			$^{207}\text{Pb}/^{206}\text{Pb}$		$^{207}\text{Pb}/^{235}\text{U}$		$^{206}\text{Pb}/^{238}\text{U}$		$^{207}\text{Pb}/^{206}\text{Pb}$		$^{207}\text{Pb}/^{235}\text{U}$		$^{206}\text{Pb}/^{238}\text{U}$		Concordance	
	Pb	Th	U	Ratio	1 σ	Ratio	1 σ	Ratio	1 σ	Age (Ma)	14	13	1287	20			
										1313	13	1286	21	97%			
1027-2-52	154	273	566	0.48	0.0867	0.0006	2.6452	0.0458	0.2210	0.0038	1355	14	1313	13	1287	20	97%
1027-2-53	131	307	470	0.65	0.0862	0.0006	2.6243	0.0454	0.2208	0.0040	1343	19	1307	13	1286	21	98%
1027-2-54	203	56	1033	0.05	0.0751	0.0005	1.8795	0.0338	0.1812	0.0031	1072	13	1074	12	1073	17	99%
1027-2-55	189	350	1004	0.35	0.0735	0.0005	1.6060	0.0190	0.1583	0.0019	1028	15	973	7	947	10	97%
1027-2-56	170	360	961	0.37	0.0708	0.0006	1.4217	0.0234	0.1456	0.0026	954	15	898	10	876	15	97%
1027-2-57	396	877	1527	0.57	0.0806	0.0007	2.2779	0.0366	0.2051	0.0034	1211	17	1205	11	1202	18	99%
1027-2-58	219	255	530	0.48	0.1128	0.0010	5.0533	0.0836	0.3244	0.0053	1856	15	1828	14	1811	26	99%
1027-2-59	114	452	460	0.98	0.0759	0.0008	1.8912	0.0362	0.1805	0.0033	1092	25	1078	13	1070	18	99%
1027-2-60	70	124	372	0.33	0.0712	0.0008	1.5670	0.0321	0.1595	0.0032	965	23	957	13	954	18	99%
1027-2-61	67	875	622	1.41	0.0559	0.0007	0.5626	0.0137	0.0728	0.0016	450	28	453	9	453	10	99%
1027-2-62	248	444	608	0.73	0.1041	0.0009	4.4631	0.0784	0.3104	0.0053	1698	15	1724	15	1743	26	98%
1027-2-63	75	47	367	0.13	0.0773	0.0006	1.9326	0.0364	0.1811	0.0035	1129	12	1092	13	1073	19	98%
1027-2-64	136	113	728	0.15	0.0744	0.0006	1.6490	0.0462	0.1599	0.0040	1054	17	989	18	956	22	96%
1027-2-65	118	329	643	0.51	0.0714	0.0006	1.4663	0.0319	0.1485	0.0032	970	17	917	13	893	18	97%
1027-2-66	97	204	289	0.70	0.0935	0.0007	3.3056	0.0381	0.2588	0.0027	1498	19	1482	9	1468	14	99%
1027-2-67	555	113	672	0.17	0.2666	0.0020	23.0685	0.3056	0.6274	0.0098	3286	11	3230	13	3139	39	97%
1027-2-68	65	387	296	1.31	0.0717	0.0007	1.4614	0.0252	0.1475	0.0022	976	14	915	10	887	12	96%
1027-2-70	111	222	625	0.35	0.0705	0.0005	1.4579	0.0231	0.1497	0.0025	943	18	913	10	899	14	98%
1027-2-71	69	238	244	0.97	0.0835	0.0009	2.3664	0.0464	0.2052	0.0040	1283	22	1233	14	1203	21	97%
1027-2-72	82	233	452	0.52	0.0708	0.0006	1.4368	0.0272	0.1468	0.0026	952	16	904	11	883	15	97%
1027-2-73	105	416	536	0.78	0.0700	0.0007	1.4358	0.0291	0.1486	0.0031	928	19	904	12	893	18	98%
1027-2-74	213	379	545	0.69	0.1053	0.0009	4.4860	0.0972	0.3079	0.0063	1720	15	1728	18	1730	31	99%
1027-2-75	55	188	296	0.64	0.0714	0.0007	1.4420	0.0248	0.1462	0.0025	969	20	907	10	880	14	96%
1027-2-76	37	151	322	0.47	0.0621	0.0008	0.8091	0.0188	0.0943	0.0020	676	25	602	11	581	12	96%
1027-2-77	109	176	644	0.27	0.0713	0.0008	1.4479	0.0302	0.1469	0.0030	969	21	909	13	884	17	97%
1027-2-78	150	140	341	0.41	0.1551	0.0014	7.2292	0.1924	0.3368	0.0086	2403	17	2140	24	1871	41	86%
1027-2-79	90	308	425	0.72	0.0705	0.0012	1.5641	0.0332	0.1606	0.0029	943	33	956	13	960	16	99%
20161028-1																	
1028-1-1	304	561	1424	0.39	0.0794	0.0008	1.9639	0.0374	0.1787	0.0032	1183	52	1103	13	1060	17	96%
1028-1-2	89	240	399	0.60	0.0782	0.0010	1.9338	0.0639	0.1780	0.0046	1152	26	1093	22	1056	25	96%
1028-1-3	577	161	891	0.18	0.1902	0.0015	13.7567	0.1548	0.5230	0.0057	2744	13	2733	11	2712	24	99%
1028-1-4	54	300	332	0.90	0.0660	0.0008	1.1209	0.0222	0.1229	0.0022	806	21	763	11	747	13	97%
1028-1-5	313	732	421	1.74	0.1649	0.0013	10.6933	0.1158	0.4690	0.0048	2506	13	2497	10	2479	21	99%
1028-1-6	33	92	158	0.58	0.0740	0.0009	1.7278	0.0292	0.1693	0.0029	1043	24	1019	11	1008	16	98%
1028-1-7	168	27	1040	0.03	0.0709	0.0006	1.4518	0.0175	0.1482	0.0017	955	19	911	7	891	10	97%
1028-1-8	42	99	237	0.42	0.0679	0.0009	1.3983	0.0299	0.1490	0.0028	866	28	888	13	895	16	99%
1028-1-9	418	492	657	0.75	0.1608	0.0015	10.5026	0.1834	0.4730	0.0080	2465	16	2480	16	2497	35	99%
1028-1-10	54	152	278	0.55	0.0724	0.0008	1.5781	0.0336	0.1581	0.0034	998	24	962	13	946	19	98%
1028-1-11	255	231	387	0.60	0.1801	0.0018	12.2404	0.1962	0.4923	0.0082	2654	17	2623	15	2580	36	98%
1028-1-12	179	200	999	0.20	0.0710	0.0007	1.5495	0.0309	0.1582	0.0032	967	25	950	12	947	18	99%
1028-1-13	111	214	352	0.61	0.0897	0.0010	3.0978	0.0674	0.2500	0.0049	1420	21	1432	17	1439	25	99%
1028-1-14	31	121	154	0.79	0.0707	0.0009	1.5712	0.0367	0.1608	0.0032	950	26	959	14	961	18	99%
1028-1-15	27	111	131	0.84	0.0689	0.0009	1.4293	0.0300	0.1504	0.0027	898	23	901	13	903	15	99%
1028-1-16	105	126	589	0.21	0.0707	0.0007	1.5556	0.0309	0.1593	0.0028	950	22	953	12	953	16	99%
1028-1-17	102	98	576	0.17	0.0717	0.0007	1.5764	0.0309	0.1595	0.0031	977	16	961	12	954	17	99%
1028-1-18	119	288	674	0.43	0.0693	0.0007	1.4069	0.0300	0.1470	0.0029	909	20	892	13	884	16	99%
1028-1-19	14	122	75	1.62	0.0642	0.0016	1.0882	0.0319	0.1229	0.0023	746	52	748	16	747	13	99%
1028-1-20	96	228	528	0.43	0.0681	0.0008	1.4084	0.0253	0.1498	0.0023	872	22	892	11	900	13	99%
1028-1-21	190	127	268	0.48	0.2306	0.0023	17.2426	0.4657	0.5404	0.0132	3057	16	2948	26	2785	55	94%
1028-1-22	174	548	597	0.92	0.0842	0.0009	2.4651	0.0383	0.2123	0.0030	1298	20	1262	11	1241	16	98%
1028-1-23	109	109	604	0.18	0.0728	0.0007	1.5830	0.0311	0.1574	0.0025	1007	20	964	12	942	14	97%
1028-1-24	340	725	1063	0.68	0.1455	0.0013	4.8074	0.0810	0.2392	0.0033	2294	16	1786	14	1383	17	74%
1028-1-25	141	205	330	0.62	0.1117	0.0015	5.0003	0.0945	0.3244	0.0048	1828	25	1819	16	1811	23	99%
1028-1-26	27	71	117	0.61	0.0769	0.0012	1.9107	0.0466	0.1800	0.0036	1120	31	1085	16	1067	19	98%
1028-1-27	22	226	149	1.51	0.0605	0.0012	0.8011	0.0227	0.0961	0.0023	620	37	597	13	591	14	98%
1028-1-28	68	391	292	1.34	0.0722	0.0009	1.5899	0.0345	0.1597	0.0033	992	25	966	14	955	18	98%
1028-1-29	198	259	468	0.55	0.1139	0.0013	5.1614	0.0887	0.3281	0.0048	1862	20	1846	15	1829	23	99%
1028-1-30	149	240	498	0.48	0.0892	0.0010	2.9055	0.0539	0.2357	0.0038	1409	21	1383	14	1364	2	

Continued Table 1

20161028-1	Elemental abundance (ppm)			$^{207}\text{Pb}/^{206}\text{Pb}$		$^{207}\text{Pb}/^{235}\text{U}$		$^{206}\text{Pb}/^{238}\text{U}$		$^{207}\text{Pb}/^{206}\text{Pb}$		$^{207}\text{Pb}/^{235}\text{U}$		$^{206}\text{Pb}/^{238}\text{U}$		Concordance	
	Pb	Th	U	Th/U	Ratio	1σ	Ratio	1σ	Ratio	1σ	Age (Ma)	1σ	Age (Ma)	1σ	Concordance		
1028-1-1	304	561	1424	0.39	0.0794	0.0008	1.9639	0.0374	0.1787	0.0032	1183	52	1103	13	1060	17	96%
1028-1-2	89	240	399	0.60	0.0782	0.0010	1.9338	0.0639	0.1780	0.0046	1152	26	1093	22	1056	25	96%
1028-1-3	577	161	891	0.18	0.1902	0.0015	13.7567	0.1548	0.5230	0.0057	2744	13	2733	11	2712	24	99%
1028-1-4	54	300	332	0.90	0.0660	0.0008	1.1209	0.0222	0.1229	0.0022	806	21	763	11	747	13	97%
1028-1-5	313	732	421	1.74	0.1649	0.0013	10.6933	0.1158	0.4690	0.0048	2506	13	2497	10	2479	21	99%
1028-1-6	33	92	158	0.58	0.0740	0.0009	1.7278	0.0292	0.1693	0.0029	1043	24	1019	11	1008	16	98%
1028-1-7	168	27	1040	0.03	0.0709	0.0006	1.4518	0.0175	0.1482	0.0017	955	19	911	7	891	10	97%
1028-1-8	42	99	237	0.42	0.0679	0.0009	1.3983	0.0299	0.1490	0.0028	866	28	888	13	895	16	99%
1028-1-9	418	492	657	0.75	0.1608	0.0015	10.5026	0.1834	0.4730	0.0080	2465	16	2480	16	2497	35	99%
1028-1-10	54	152	278	0.55	0.0724	0.0008	1.5781	0.0336	0.1581	0.0034	998	24	962	13	946	19	98%
1028-1-11	255	231	387	0.60	0.1801	0.0018	12.2404	0.1962	0.4923	0.0082	2654	17	2623	15	2580	36	98%
1028-1-12	179	200	999	0.20	0.0710	0.0007	1.5495	0.0309	0.1582	0.0032	967	25	950	12	947	18	99%
1028-1-13	111	214	352	0.61	0.0897	0.0010	3.9078	0.0674	0.2500	0.0049	1420	21	1432	17	1439	25	99%
1028-1-14	31	121	154	0.79	0.0707	0.0009	1.5712	0.0367	0.1608	0.0032	950	26	959	14	961	18	99%
1028-1-15	27	111	131	0.84	0.0689	0.0009	1.4293	0.0300	0.1504	0.0027	898	23	901	13	903	15	99%
1028-1-16	105	126	589	0.21	0.0707	0.0007	1.5556	0.0309	0.1593	0.0028	950	22	953	12	953	16	99%
1028-1-17	102	98	576	0.17	0.0717	0.0007	1.5764	0.0309	0.1595	0.0031	977	16	961	12	954	17	99%
1028-1-18	119	288	674	0.43	0.0693	0.0007	1.4069	0.0300	0.1470	0.0029	909	20	892	13	884	16	99%
1028-1-19	14	122	75	1.62	0.0642	0.0016	1.0882	0.0319	0.1229	0.0023	746	52	748	16	747	13	99%
1028-1-20	96	228	528	0.43	0.0681	0.0008	1.4084	0.0253	0.1498	0.0023	872	22	892	11	900	13	99%
1028-1-21	190	127	268	0.48	0.2306	0.0023	17.2426	0.4657	0.5404	0.0132	3057	16	2948	26	2785	55	94%
1028-1-22	174	548	597	0.92	0.0842	0.0009	2.4651	0.0383	0.2123	0.0030	1298	20	1262	11	1241	16	98%
1028-1-23	109	109	604	0.18	0.0728	0.0007	1.5830	0.0311	0.1574	0.0025	1007	20	964	12	942	14	97%
1028-1-24	340	725	1063	0.68	0.1455	0.0013	4.8074	0.0810	0.2392	0.0033	2294	16	1786	14	1383	17	74%
1028-1-25	141	205	330	0.62	0.1117	0.0015	5.0003	0.0945	0.3244	0.0048	1828	25	1819	16	1811	23	99%
1028-1-26	27	71	117	0.61	0.0769	0.0012	1.9107	0.0466	0.1800	0.0036	1120	31	1085	16	1067	19	98%
1028-1-27	22	226	149	1.51	0.0605	0.0012	0.8011	0.0227	0.0961	0.0023	620	37	597	13	591	14	98%
1028-1-28	68	391	292	1.34	0.0722	0.0009	1.5899	0.0345	0.1597	0.0033	992	25	966	14	955	18	98%
1028-1-29	198	259	468	0.55	0.1139	0.0013	5.1614	0.0887	0.3281	0.0048	1862	20	1846	15	1829	23	99%
1028-1-30	149	240	498	0.48	0.0892	0.0010	2.9055	0.0539	0.2357	0.0038	1409	21	1383	14	1364	20	98%
1028-1-31	294	756	782	0.97	0.0992	0.0009	3.6407	0.0517	0.2657	0.0031	1609	18	1558	11	1519	16	97%
1028-1-32	497	1186	928	1.28	0.1327	0.0013	6.4776	0.1600	0.3532	0.0080	2200	17	2043	22	1950	38	95%
1028-1-33	119	319	629	0.51	0.0692	0.0008	1.4135	0.0213	0.1480	0.0018	906	24	895	9	890	10	99%
1028-1-34	159	201	236	0.85	0.1659	0.0015	10.7711	0.2013	0.4700	0.0079	2516	15	2504	17	2484	35	99%
1028-1-35	89	121	213	0.57	0.1083	0.0010	4.6427	0.0616	0.3106	0.0034	1772	17	1757	11	1743	17	99%
1028-1-36	152	313	398	0.79	0.0968	0.0017	3.6005	0.1010	0.2692	0.0040	1565	33	1550	22	1537	20	99%
1028-1-37	58	173	139	1.24	0.0997	0.0010	3.6883	0.0764	0.2683	0.0053	1618	19	1569	17	1532	27	97%
1028-1-38	61	97	326	0.30	0.0710	0.0012	1.4652	0.0367	0.1493	0.0024	967	33	916	15	897	13	97%
1028-1-39	143	325	372	0.88	0.0998	0.0010	3.6748	0.0764	0.2667	0.0049	1620	180	1566	17	1524	25	97%
1028-1-40	72	134	388	0.35	0.0711	0.0009	1.4507	0.0350	0.1479	0.0032	961	25	910	15	889	18	97%
1028-1-41	35	48	238	0.20	0.0648	0.0009	1.926	0.0237	0.1221	0.0019	766	27	750	12	743	11	99%
1028-1-42	79	50	183	0.27	0.1210	0.0012	5.7893	0.1235	0.3461	0.0060	1972	17	1945	18	1916	29	98%
1028-1-43	29	158	229	0.69	0.0618	0.0009	0.8165	0.0149	0.0958	0.0012	665	31	606	8	590	7	97%
1028-1-44	40	98	49	2.00	0.1644	0.0018	10.5917	0.1644	0.4668	0.0056	2501	19	2488	14	2470	25	99%
1028-1-45	51	116	279	0.42	0.0708	0.0008	1.4562	0.0362	0.1490	0.0033	950	23	912	15	895	18	98%
1028-1-46	111	621	675	0.92	0.0645	0.0006	1.0835	0.0207	0.1219	0.0025	761	25	745	10	742	14	99%
1028-1-47	65	175	317	0.55	0.0726	0.0007	1.5919	0.0351	0.1588	0.0033	1006	25	967	14	950	19	98%
1028-1-48	346	727	481	1.51	0.1630	0.0023	10.4867	0.3752	0.4654	0.0137	2487	24	2479	33	2463	60	99%
1028-1-49	74	55	359	0.15	0.0752	0.0005	1.8628	0.0335	0.1796	0.0033	1074	13	1068	12	1065	18	99%
1028-1-50	95	418	379	1.10	0.0761	0.0006	1.8754	0.0306	0.1789	0.0033	1098	21	1072	11	1061	18	98%
1028-1-52	305	247	445	0.56	0.1841	0.0012	13.1817	0.1941	0.5187	0.0080	2690	11	2693	14	2694	34	99%
1028-1-53	123	258	408	0.63	0.0893	0.0007	2.8919	0.0416	0.2348	0.0035	1410	15	1380	11	1360	18	98%
1028-1-54	189	645	811	0.80	0.0779	0.0013	1.9231	0.0468	0.1786	0.0038	1146	28	1089	16	1059	21	97%
1028-1-55	31	403	193	2.09	0.0614	0.0027	0.8362	0.0371	0.0987	0.0023	654	90	617	21	606	14	98%
1028-1-56	88	321	227	1.42	0.0986	0.0009	3.6291	0.0696	0.2666	0.0052	1598	18	1556	15	1523	26	97%
1028-1-57	340	773	1323	0.58	0.0891	0.0008	2.5376	0.0407	0.2060	0.0029	1406	17	1283	12	1207	16	93%
1028-1-58	186	246	911	0.27	0.0781	0.0007	1.9223	0.0341	0.1782	0.0032	1150	17	1089	12	1057	17	97%
1028-1-59	167	309	331	0.93	0.1492	0.0017	7.4448	0.1229	0.3613	0.0057	2339	25	2166	15	1988	27	91%
1028-1-60	333	2068	1198	1.73	0.2474	0.0136	5.3815	0.4290	0.1494	0.0045	3168	87	1882	68	898		

Continued Table 1

20161028-1	Elemental abundance (ppm)			$^{207}\text{Pb}/^{206}\text{Pb}$		$^{207}\text{Pb}/^{235}\text{U}$		$^{206}\text{Pb}/^{238}\text{U}$		$^{207}\text{Pb}/^{206}\text{Pb}$		$^{207}\text{Pb}/^{235}\text{U}$		$^{206}\text{Pb}/^{238}\text{U}$		Concordance	
	Pb	Th	U	Ratio	1 σ	Ratio	1 σ	Ratio	1 σ	Age (Ma)	1 σ	Age (Ma)	1 σ	Age (Ma)			
1028-1-71	21	244	173	1.41	0.0600	0.0012	0.6564	0.0227	0.0789	0.0019	611	44	512	14	490	11	95%
1028-1-72	79	44	184	0.24	0.1228	0.0016	5.8818	0.0803	0.3473	0.0046	1998	23	1959	12	1922	22	98%
1028-1-73	56	177	265	0.67	0.0717	0.0007	1.5935	0.0303	0.1610	0.0030	989	17	968	12	962	17	99%
1028-1-74	296	2081	1687	1.23	0.0667	0.0006	1.1205	0.0181	0.1215	0.0019	829	21	763	9	739	11	96%
1028-1-75	52	251	256	0.98	0.0701	0.0008	1.4298	0.0290	0.1478	0.0029	931	24	901	12	889	16	98%
1028-1-76	76	668	705	0.95	0.0584	0.0006	0.6469	0.0123	0.0802	0.0015	543	24	507	8	497	9	98%
1028-1-77	44	80	224	0.36	0.0754	0.0009	1.7584	0.0372	0.1687	0.0033	1080	25	1030	14	1005	18	97%
1028-1-78	116	350	1042	0.34	0.0615	0.0008	0.8330	0.0200	0.0979	0.0021	657	26	615	11	602	12	97%
1028-1-79	222	167	396	0.42	0.1560	0.0016	9.6939	0.1946	0.4496	0.0089	2413	18	2406	18	2393	39	99%
1028-1-80	224	474	531	0.89	0.1068	0.0015	4.6130	0.0940	0.3127	0.0063	1746	26	1752	17	1754	31	99%
1028-1-81	108	162	329	0.49	0.1011	0.0015	3.6975	0.0996	0.2640	0.0051	1644	28	1571	22	1511	26	96%
1028-1-82	148	183	230	0.79	0.1633	0.0015	10.5972	0.1560	0.4696	0.0063	2500	15	2488	14	2482	28	99%
1028-1-83	59	356	403	0.88	0.0798	0.0011	1.1562	0.0208	0.1047	0.0013	1192	28	780	10	642	8	80%
1028-1-84	202	248	678	0.37	0.0919	0.0008	3.1269	0.0463	0.2462	0.0034	1466	17	1439	11	1419	17	98%
1028-1-85	885	1463	2975	0.49	0.1327	0.0065	4.3532	0.2814	0.2322	0.0042	2200	85	1704	53	1346	22	76%
1028-1-86	61	239	269	0.89	0.0752	0.0008	1.7618	0.0407	0.1693	0.0034	1076	21	1032	15	1008	19	97%
1028-1-87	250	296	994	0.30	0.0879	0.0008	2.5378	0.0418	0.2093	0.0036	1381	17	1283	12	1225	19	95%
1028-1-88	92	177	355	0.50	0.0869	0.0009	2.5045	0.0795	0.2083	0.0059	1358	25	1273	23	1220	31	95%
1028-1-89	30	252	290	0.87	0.0588	0.0009	0.6322	0.0143	0.0779	0.0015	561	31	497	9	484	9	97%
1028-1-90	37	165	139	1.18	0.0781	0.0018	1.9411	0.0531	0.1799	0.0029	1150	45	1095	18	1066	16	97%
1028-1-91	33	143	154	0.93	0.0720	0.0009	1.5633	0.0338	0.1573	0.0029	987	24	956	13	942	16	98%
1028-1-92	32	338	288	1.17	0.0585	0.0009	0.6244	0.0135	0.0774	0.0014	550	33	493	8	481	8	97%
1028-1-93	18	269	140	1.92	0.0567	0.0009	0.6153	0.0143	0.0784	0.0012	480	40	487	9	487	7	99%
1028-1-94	41	97	192	0.51	0.0755	0.0009	1.7555	0.0314	0.1684	0.0025	1083	22	1029	12	1003	14	97%
1028-1-95	61	270	370	0.73	0.0676	0.0008	1.1499	0.0216	0.1232	0.0018	855	24	777	10	749	10	96%
1028-1-96	49	167	255	0.65	0.0700	0.0007	1.4283	0.0192	0.1478	0.0014	928	22	901	8	888	8	98%

using an X-ray fluorescence spectrometer (XRF-1500) at the National geological experiment testing center, Chinese Academy of Geological Sciences (CAGS). The analytical precision is generally better than 5% for all elements. Trace element abundances were measured using a Plasma mass spectrometer(PE300D) in the National geological experiment testing center, Chinese Academy of Geological Sciences (CAGS), The analysis results were in parts per million.

5 Analytical Results

5.1 U-Pb ages of detrital zircons

A total of 260 detrital zircons analyses were undertaken. Zircon U-Pb isotopic compositions are presented in Table 1. Uncertainties on individual analyses in the data table and concordia plots are presented at 1 σ . Most of all analyses are shown on concordia plots (Fig. 5), and ages less than 1000 Ma are based on the $^{206}\text{Pb}/^{238}\text{U}$ ratio whereas older ages are based on the $^{206}\text{Pb}/^{207}\text{Pb}$ ratio. Ages calculated for multiple grains are quoted with 95% confidence limits.

5.1.1 Sample 20161026-2

Eighty-five U-Pb spots were analysed on 85 zircon grains, of which 79 analyses are concordant. The detrital zircons from these samples have euhedral–subhedral morphology, implying that their primary sources were not far from the depositional site. All of the Th/U values are greater than 0.1, which indicate that zircons in the Tianmashan Formation are mostly magmatic origin (Belousova et al., 2002; Corfu et al., 2003).

The concordant zircon U-Pb data from Tianmashan Formation define the ages in the range of 523 to 3576 Ma

(Fig. 5), with four main age populations of 523–792 Ma, 904–1489 Ma, 1607–1891 Ma, 2031–2842 Ma.

5.1.2 Sample 20161027-2

Seventy-nine U-Pb spots were analysed on 79 zircon grains, of which 75 analyses are concordant. The detrital zircons from these samples have euhedral–subhedral morphology, implying that their primary sources were not far from the depositional site. All of the Th/U values are greater than 0.1, which indicate that zircons in the Tianmashan Formation are mostly magmatic origin (Belousova et al., 2002; Corfu et al., 2003).

The concordant zircon U-Pb data from Tianmashan Formation define the ages in the range of 453 to 3286 Ma (Fig. 5), with four main age populations of 453–661 Ma, 876–1283 Ma, 1342–1855 Ma and 2065–2632 Ma.

5.1.3 Sample 20161028-1

Ninety-six U-Pb spots were analysed on 96 zircon grains, of which 91 analyses are concordant. The detrital zircons from these samples are euhedral and subhedral with clear oscillatory zoning, implying that their primary sources were not far from the depositional site. All of the Th/U values are greater than 0.1, which indicate that zircons in the Tianmashan Formation are mostly magmatic origin (Belousova et al., 2002; Corfu et al., 2003).

The concordant zircon U-Pb data from Tianmashan Formation define the ages in the range of 481 to 3057 Ma (Fig. 5), with four main age populations of 481–749 Ma, 884–1183 Ma, 1298–1643 Ma, 1746–1998 Ma and 2200–2744 Ma.

5.2 Whole-rock geochemistry

Geochemistry compositions are presented in Table 2.

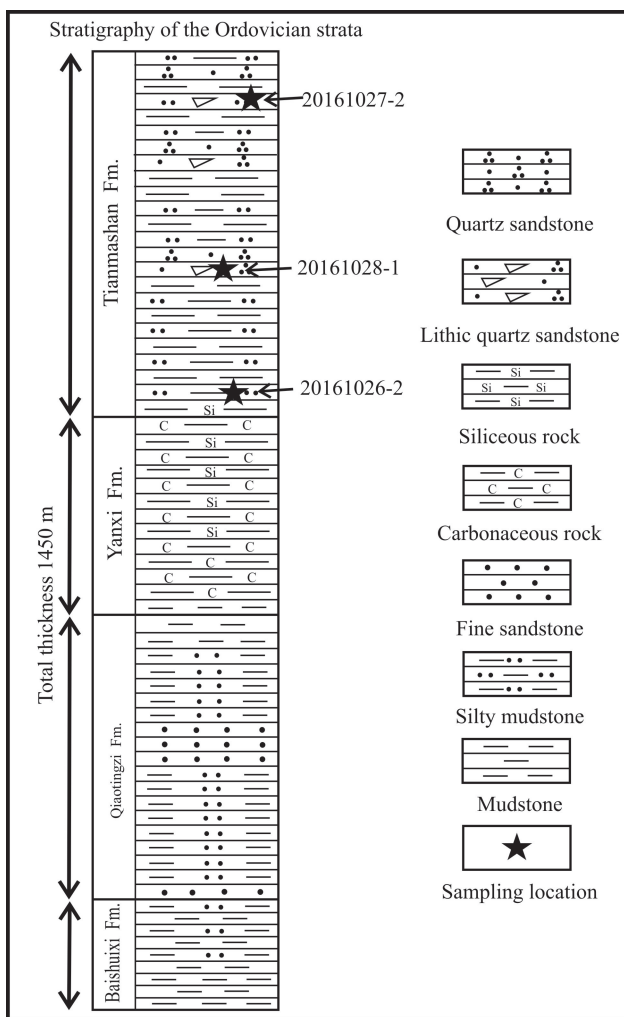


Fig. 4. Stratigraphic column of the Ordovician strata, Hunan province, South China.

The sedimentary rock samples from Baishuixi and Qiaotingzi Formations have lower SiO_2 (56.23–72.50 wt%), higher Al_2O_3 (13.14–21.50 wt%), $\text{Fe}_{2\text{O}}^{\text{T}}$ (3.84–9.65 wt%), and TiO_2 (0.51–0.79 wt%), implying that the sedimentary rocks possess immature lithic varieties and mafic components. The total contents of rare earth elements (REE) in the sedimentary rocks vary from 135 to 308 ppm, PAAS-normalized REE patterns indicate that sedimentary rocks have weaker enrichment of light REE (Fig. 6). The $(\text{La}/\text{Yb})_{\text{N}}$ values vary from 0.65 to 2.84. Most samples show weak negative or positive Eu anomalies ($\text{Eu}/\text{Eu}^* = 0.73$ –1.03). Overall, REE patterns of these sedimentary rocks are similar to those of the Post-Archean Australia shale (PAAS). The samples display moderate depletion of Gd, Sr and Mo and enrichment of Rb, Ba and Bi (Fig. 6). Compatible element contents of these sedimentary rocks are similar to the Post-Archean Australia shales (PAAS), but Sr, Gd and Mo is poor and Ba is enriched relative to the PAAS. Because Ba is easily absorbed and Sr is easily leached during the weathering, so it can be suggested that the sedimentary rocks in this paper experienced stronger weathering than the PAAS.

6 Discussion

6.1 Provenance and depositional environment of the sedimentary rocks

6.1.1 Lower Ordovician

The Chemical Index of Alteration (CIA) is a helpful argument to evaluate the weathering characteristic of the provenance of the sedimentary rocks (Nesbitt et al., 1982; Fedo et al., 2003). The Baishuixi and Qiaotingzi Formations have large scale CIA values (54 to 83, with average of 80), showing a moderate to strong weathering process. If the plagioclases in sedimentary rocks were completely corroded, the rocks will be plotted close to the A–K boundary. In addition, as weathering increases, K removes from the K-feldspar, and the rock compositions evolve toward the Al_2O_3 end in the A–CN–K diagram (Fig. 7). The intersection of weathering evolution line and the plagioclase K-feldspar join can exhibit the proportion of plagioclase and K-feldspar in the source rocks, and more accurately restrain the rock types of provenance. The points of intersection of the samples in this study mostly plot in the area of the upper crust and granites, suggesting a provenance of felsic rocks (Fig. 7).

In the F1–F2 provenance discrimination diagram (Fig. 7), sediment sources are divided into four areas, including felsic igneous, intermediate igneous, mafic igneous and quartzose sedimentary provenances. All sedimentary rocks (except one) of the Baishuixi and Qiaotingzi Formations fall in the quartzose sedimentary provenance field, suggesting that their sediments of lower Ordovician (Baishuixi and Qiaotingzi Formation) mainly derived from recycled sedimentary rocks.

Unimodal cross-bedding is clearly observable in fine-grained sandstone rocks of the Baishuixi and Qiaotingzi Formations (Fig. 3), the Paleocurrent directions demonstrate that sediments were derived from the present-day north–westerly direction (Fig. 9). Base on the geochemical features, source composition and cross-bedding of the Baishuixi and Qiaotingzi Formations, suggesting that the Yangtze Block was the probable source for the lower Ordovician strata.

Bhatia (1983) proposed that the sediments deposited in continental island arc, passive continental margin, oceanic island arc and active continental margin have obviously distinct geochemical features, which could be used to effectively analyze the different tectonic environment. In the discrimination diagrams of $\text{K}_2\text{O}/\text{Na}_2\text{O}$ – SiO_2 , most of the samples of the Baishuixi and Qiaotingzi Formations fall in the field of passive continental margin sedimentary basin (Fig. 8). Furthermore, trace elements, such as REE, Y, Th, Zr, Hf and Sc, are relatively immobile related to the major elements (McLennan et al., 1993; Bai et al., 2007). Thus, the immobile elements can be used to effectively identify the tectonic settings. Majority of the samples plot in or near the PM (passive continental margin) area in the La–Th–Sc diagram (Fig. 8), implying that the sediments were deposited in a passive continental margin setting.

6.1.2 Upper Ordovician

Comparing the age spectra of detrital zircons from the

Table 2 Major (wt%) and trace element (ppm) data for sandstone samples from the Baishuixi and Qiaotingzi formations

Sample	BSX1	BSX2	BSX3	BSX4	BSX5	BSX6	BSX7	BSX8	BSX9	BSX10	BSX11	BSX12
SiO ₂	65.9	57.1	66.6	68.5	67.6	62.5	56.2	59.1	57.5	62.1	58.27	59.4
Al ₂ O ₃	15.9	13.1	15.0	15.8	15.0	18.67	21.01	18.66	21.50	18.27	19.99	17.79
CaO	0.15	7.43	0.19	0.10	0.08	0.08	0.08	0.14	0.07	0.08	0.23	0.31
Fe ₂ O ₃	4.49	2.62	4.88	4.41	6.21	7.33	2.84	6.98	4.81	3.33	4.10	5.09
FeO	1.13	2.35	0.92	0.48	0.48	0.70	4.94	1.49	1.63	3.57	2.64	3.22
K ₂ O	3.40	3.04	3.38	3.65	3.64	3.56	3.88	3.91	4.83	3.76	4.01	2.92
MgO	2.47	2.79	2.31	1.13	0.99	0.77	3.54	3.12	3.14	2.65	2.58	3.33
MnO	0.07	0.07	0.08	0.08	0.04	0.07	0.10	0.09	0.05	0.07	0.05	0.17
Na ₂ O	0.23	0.55	0.50	0.01	0.01	0.05	0.11	0.72	0.14	0.04	0.06	0.44
P ₂ O ₅	0.08	0.13	0.14	0.11	0.11	0.08	0.06	0.07	0.06	0.06	0.09	0.08
TiO ₂	0.61	0.51	0.58	0.64	0.62	0.65	0.76	0.71	0.76	0.63	0.74	0.66
CO ₂	0.17	6.43	0.51	0.34	0.34	0.26	0.34	0.26	0.34	0.26	0.26	0.51
H ₂ O	4.35	3.57	4.06	4.05	3.99	4.78	5.21	4.03	4.69	4.49	5.22	5.36
LOI	4.70	9.87	4.34	4.29	4.24	5.21	5.25	4.11	4.87	4.50	5.26	5.73
Li	54.7	38.0	31.1	46.9	32.7	33.3	51.2	35.3	35.7	31.8	39.5	60.9
Be	4.12	3.30	3.55	3.89	3.75	4.69	4.61	4.15	5.09	4.10	5.03	3.97
Cr	99.2	73.8	92.4	95.0	96.6	85.1	103	93.6	113	92.6	109	95.6
Mn	530	562	593	581	337	508	775	714	417	517	414	1318
Co	14.8	11.9	17.4	11.8	10.2	13.6	21.7	21.6	19.3	17.7	18.1	21.0
Ni	50.9	38.4	70.3	34.8	42.1	54.4	58.7	54.2	52.4	49.1	47.9	53.9
Cu	42.4	37.1	40.6	47.2	49.5	26.8	17.8	0.18	4.89	0.73	58.1	45.3
Zn	113	105	112	76.9	89.7	79.7	140	104	118	116	129	135
Ga	24.5	19.5	23.1	23.7	23.3	27.3	31.5	28.1	31.9	26.0	29.7	27.0
Rb	159	127	141	153	167	149	76.6	156	236	181	175	142
Sr	12.5	126	14.4	8.24	9.43	25.4	31.4	47.6	55.5	32.5	22.9	38.7
Mo	1.47	1.16	1.70	1.06	1.96	0.05	0.08	0.06	0.05	0.05	0.13	0.14
Cd	0.26	0.23	0.63	0.30	0.31	0.05	0.09	0.05	0.05	0.20	0.07	0.05
In	0.07	0.06	0.07	0.07	0.06	0.08	0.10	0.08	0.09	0.07	0.09	0.08
Cs	7.33	5.90	6.51	7.46	7.69	7.43	6.46	8.90	11.3	7.47	7.26	5.16
Ba	2012	1856	2012	2089	2116	919	923	979	1179	670	10520	1609
Tl	0.72	0.59	0.75	0.78	0.80	0.63	0.68	0.74	0.92	0.76	0.68	0.58
Pb	15.8	12.2	27.3	12.2	13.1	4.35	5.34	9.07	8.57	4.44	22.2	5.36
Bi	0.38	0.33	0.38	0.34	0.35	0.07	0.05	0.40	0.40	0.13	0.44	0.07
Th	16.2	13.0	15.2	15.1	15.8	15.3	19.4	18.0	17.1	17.0	17.9	18.6
U	2.74	2.30	3.31	2.91	3.94	1.57	1.84	1.80	2.15	2.13	3.08	2.78
Nb	11.9	9.78	11.2	12.1	11.8	12.5	15.4	13.9	13.8	11.5	13.7	13.3
Ta	1.01	0.81	0.94	0.98	0.97	1.01	1.24	1.12	1.10	0.98	1.11	1.11
Zr	87.7	72.2	80.6	94.2	91.0	81.0	101	102	89.9	78.6	92.2	101
Hf	2.98	2.40	2.71	3.12	3.10	2.81	3.41	3.45	2.99	2.71	3.09	3.34
Sn	3.52	2.83	3.40	3.48	3.34	3.48	4.35	3.80	3.87	3.38	3.74	3.61
Sb	1.57	1.10	2.25	1.04	4.24	0.42	0.50	1.10	1.11	0.56	0.87	0.33
Ti	3971	3292	3730	4090	3952	4172	4926	4481	4759	3783	4603	4160
W	1.94	1.57	1.62	1.79	1.76	1.95	2.50	2.20	2.34	1.85	2.23	2.12
As	7.85	6.65	15.1	8.08	9.78	0.76	0.86	0.99	0.97	0.83	10.1	1.21
V	198	144	163	143	140	105	112	117	124	117	120	94.6
La	35.5	33.5	37.2	31.4	33.0	33.4	48.9	57.1	95.2	88.7	46.9	46.6
Ce	64.5	64.1	65.7	57.6	62.3	43.0	95.0	101	92.9	107	94.2	95.7
Pr	7.74	7.60	8.37	7.19	7.66	7.52	11.0	12.5	16.4	17.1	10.6	10.2
Nd	31.6	31.6	34.4	30.0	31.4	30.6	39.9	46.3	60.7	62.0	37.6	36.8
Sm	5.24	5.43	6.07	5.04	5.54	5.32	7.33	8.68	11.0	10.8	7.04	7.12
Eu	0.96	1.06	1.18	0.90	1.02	1.06	1.37	1.67	2.11	1.98	1.31	1.37
Gd	4.25	4.90	6.17	4.08	4.85	4.54	5.72	7.46	8.39	7.32	6.41	6.03
Tb	0.78	0.85	1.09	0.73	0.87	0.81	0.99	1.29	1.39	1.25	1.13	1.09
Dy	3.87	4.06	5.54	3.76	4.24	3.98	4.63	6.02	5.91	5.20	5.42	5.21
Ho	0.79	0.82	1.12	0.76	0.87	0.79	0.87	1.18	1.05	0.97	1.07	1.06
Er	2.34	2.42	3.02	2.18	2.51	2.23	2.53	3.27	2.78	2.70	2.96	3.04
Tm	0.35	0.34	0.42	0.32	0.37	0.32	0.36	0.45	0.39	0.37	0.41	0.42
Yb	2.23	2.26	2.72	2.03	2.38	2.12	2.38	2.93	2.47	2.49	2.70	2.71
Lu	0.33	0.34	0.41	0.30	0.35	0.31	0.35	0.43	0.37	0.36	0.42	0.40
Sc	15.5	12.0	13.8	14.3	15.3	15.2	17.9	16.6	20.4	16.7	20.0	16.9
Y	22.4	24.3	34.1	21.3	24.8	19.9	23.4	33.2	26.0	24.5	29.8	29.7
Sample	BSX13	BSX14	QTZ1	QTZ2	QTZ3	QTZ4	QTZ5	QTZ6	QTZ7	QTZ8	QTZ9	QTZ10
SiO ₂	61.4	62.3	58.6	59.4	57.3	59.8	71.9	72.5	71.4	71.0	62.2	65.0
Al ₂ O ₃	17.93	17.77	19.85	19.12	21.11	19.10	13.55	13.50	13.84	13.63	17.83	16.3
CaO	0.20	0.19	0.23	0.20	0.12	0.08	0.13	0.08	0.08	0.08	0.27	0.29
Fe ₂ O ₃	2.61	3.44	1.91	0.85	2.93	3.26	3.23	2.35	2.50	2.66	4.86	4.52
FeO	3.79	2.50	5.30	6.52	4.08	3.50	0.84	1.35	1.63	1.56	1.42	1.13
K ₂ O	3.29	3.30	3.77	3.29	4.00	3.42	3.12	3.05	3.37	3.14	4.06	3.81
MgO	3.24	2.96	3.22	3.58	2.97	3.33	1.96	1.86	2.00	1.98	2.17	2.16
MnO	0.14	0.15	0.07	0.09	0.11	0.04	0.03	0.04	0.03	0.03	0.04	0.02
Na ₂ O	1.50	1.27	0.71	1.10	0.31	0.39	0.04	0.01	0.01	0.01	0.50	0.31
P ₂ O ₅	0.13	0.11	0.09	0.10	0.07	0.09	0.05	0.03	0.06	0.06	0.11	0.10

Continued Table 2

Sample	BSX13	BSX14	QTZ1	QTZ2	QTZ3	QTZ4	QTZ5	QTZ6	QTZ7	QTZ8	QTZ9	QTZ10
TiO ₂	0.72	0.73	0.75	0.71	0.77	0.71	0.62	0.61	0.61	0.60	0.79	0.63
CO ₂	0.34	0.26	0.34	0.26	0.26	0.34	0.26	0.26	0.43	0.77	0.26	0.17
H ₂ O	4.10	4.28	4.65	4.32	5.38	5.13	4.13	3.92	3.97	4.12	4.83	4.80
LOI	4.28	4.56	4.49	4.07	5.52	5.52	4.21	3.92	4.48	4.20	5.14	4.98
Li	49.6	42.8	54.7	63.3	47.5	50.1	31.7	30.5	36.1	35.1	29.1	31.3
Be	4.57	4.31	4.45	4.39	5.14	4.33	3.07	2.70	3.32	2.93	3.85	5.19
Cr	100	99.7	111	107	118	108	72.6	76.7	79.3	77.8	110	86.0
Mn	1139	1216	527	736	895	327	244	297	243	226	284	166
Co	32.8	18.4	13.8	22.0	18.6	19.7	13.8	10.4	12.3	8.93	17.1	9.42
Ni	57.7	49.5	49.9	54.7	60.8	48.7	45.7	61.5	98.7	96.0	53.9	44.8
Cu	22.8	32.1	24.6	59.5	70.9	33.8	109	93.0	87.1	92.5	38.3	41.8
Zn	123	123	137	135	156	146	125	182	292	284	161	129
Ga	27.9	27.1	29.2	28.9	32.5	28.6	23.1	22.5	22.0	21.8	28.1	26.4
Rb	164	166	185	165	199	178	156	156	159	155	207	209
Sr	61.4	55.3	50.9	59.2	35.5	29.7	15.9	17.5	20.7	21.8	31.6	27.4
Mo	0.56	0.61	0.06	0.05	0.11	0.12	0.11	1.39	0.39	0.48	0.40	1.05
Cd	0.39	0.38	0.08	0.09	0.16	0.18	0.09	0.34	0.56	0.52	0.56	0.22
In	0.07	0.08	0.08	0.09	0.10	0.08	0.07	0.07	0.06	0.06	0.09	0.09
Cs	4.79	4.82	4.87	4.02	5.06	4.16	6.91	5.75	6.67	6.39	8.42	11.5
Ba	936	908	1468	1112	1369	893	569	530	543	542	853	912
Tl	0.64	0.65	0.71	0.62	0.74	0.64	0.69	0.65	0.69	0.71	0.90	0.89
Pb	27.1	25.9	7.97	4.67	5.59	13.4	30.6	36.0	66.7	59.6	27.6	27.6
Bi	0.42	0.35	0.33	0.07	0.09	0.35	0.05	0.39	0.20	0.31	0.50	0.64
Th	18.2	18.5	16.6	18.2	20.6	17.3	18.2	17.3	17.8	17.6	21.0	22.9
U	3.16	2.58	2.21	1.76	2.46	2.48	2.16	2.56	3.12	3.18	4.03	4.43
Nb	14.4	14.4	13.4	13.6	15.4	13.5	19.9	14.4	13.1	13.2	17.0	16.4
Ta	1.17	1.17	1.06	1.07	1.22	1.07	1.06	1.10	1.03	1.03	1.35	1.42
Zr	140	137	79.8	89.5	105	90.5	155	170	159	157	175	170
Hf	3.83	3.81	2.76	3.04	3.43	3.08	4.29	4.50	4.29	4.35	4.79	5.11
Sn	3.72	3.78	3.47	3.61	4.02	3.47	3.51	3.31	3.28	3.20	4.40	4.84
Sb	4.16	2.32	0.75	0.26	0.38	0.60	0.38	1.27	1.50	2.16	0.67	1.24
Ti	4566	4496	4718	4432	5129	4468	3858	3971	3862	3770	5180	4016
W	1.74	1.78	1.91	1.93	2.06	1.83	2.31	2.54	2.50	2.49	2.15	3.49
As	23.8	13.8	3.62	0.95	7.35	9.75	2.51	16.1	10.5	12.2	8.31	7.70
V	101	104	119	101	130	116	89.4	99.2	109	104	135	109
La	47.6	47.5	48.6	53.2	54.0	51.0	49.2	45.7	52.8	51.2	58.3	57.6
Ce	97.5	97.4	101	107	109	84.5	93.4	82.9	105	105	111	106
Pr	10.9	10.5	10.8	11.4	11.6	10.6	10.1	9.77	11.3	11.1	12.3	12.9
Nd	40.2	37.7	38.1	40.6	40.5	43.2	37.7	39.4	40.6	39.2	44.4	48.4
Sm	8.11	7.46	7.47	7.66	7.25	6.92	6.28	6.47	7.79	7.57	8.22	10.0
Eu	1.55	1.46	1.49	1.50	1.35	1.35	1.12	1.20	1.40	1.34	1.52	1.51
Gd	7.06	6.50	6.23	6.53	5.84	5.85	5.25	5.49	6.65	6.56	7.02	9.30
Tb	1.23	1.15	1.09	1.17	1.08	1.03	0.99	0.95	1.17	1.13	1.26	1.61
Dy	5.97	5.71	5.28	5.66	5.09	4.80	4.82	4.68	5.80	5.50	6.21	7.81
Ho	1.18	1.11	1.04	1.13	1.03	0.99	1.03	0.92	1.15	1.11	1.24	1.55
Er	3.42	3.23	2.93	3.25	2.91	2.67	3.16	2.59	3.44	3.23	3.62	4.47
Tm	0.47	0.46	0.41	0.45	0.41	0.39	0.49	0.38	0.49	0.46	0.52	0.62
Yb	3.09	3.08	2.68	2.93	2.77	2.49	3.35	2.51	3.17	3.09	3.34	4.09
Lu	0.48	0.45	0.41	0.43	0.42	0.37	0.54	0.37	0.49	0.46	0.51	0.62
Sc	17.1	16.9	19.7	18.5	21.1	18.8	13.7	14.1	14.8	14.5	18.9	16.1
Y	33.8	32.5	28.5	32.7	28.6	27.9	29.5	25.6	32.9	30.6	36.5	45.4
Sample	QTZ11	QTZ12	QTZ13	QTZ14	QTZ15	QTZ16	QTZ17	QTZ18	QTZ19	QTZ20		
SiO ₂	56.8	61.6	62.1	63.4	59.8	58.8	57.2	58.6	58.1	57.0		
Al ₂ O ₃	18.47	18.25	19.35	16.61	18.31	18.93	18.94	18.30	19.68	20.35		
CaO	0.25	0.28	0.07	0.26	0.23	0.11	0.24	1.09	0.14	0.07		
Fe ₂ O ₃	1.82	0.81	3.88	3.06	2.13	4.31	3.03	0.66	4.14	2.96		
FeO	6.74	4.65	1.13	2.86	4.29	2.57	6.02	5.66	3.00	4.44		
K ₂ O	2.46	3.23	3.87	3.02	3.47	3.52	3.43	3.25	3.89	3.79		
MgO	5.01	3.36	2.32	3.14	4.12	3.60	3.78	4.02	3.38	3.89		
MnO	0.09	0.11	0.06	0.09	0.10	0.10	0.11	0.17	0.08	0.09		
Na ₂ O	2.07	2.28	0.10	1.18	0.93	0.59	0.65	1.36	0.53	0.02		
P ₂ O ₅	0.10	0.11	0.06	0.10	0.11	0.09	0.12	0.10	0.09	0.06		
TiO ₂	0.66	0.70	0.77	0.62	0.68	0.68	0.71	0.69	0.74	0.76		
CO ₂	0.34	0.26	0.34	0.34	0.26	0.34	0.17	1.46	0.34	0.26		
H ₂ O	4.66	3.58	5.10	4.32	4.68	5.35	5.02	3.99	5.15	5.42		
LOI	4.46	3.48	5.44	4.39	4.63	5.67	4.86	5.00	5.35	5.49		
Li	54.6	38.7	27.1	40.7	46.8	40.2	47.8	50.5	41.3	63.7		
Be	5.32	5.41	5.39	3.55	4.53	5.05	4.54	4.35	5.21	4.89		
Cr	98.8	101	102	90.8	99.7	103	102	99.8	93.6	96.8		
Mn	725	884	433	701	784	774	865	1377	658	731		
Co	25.7	18.6	15.5	16.9	17.2	18.2	19.4	19.9	22.6	24.4		
Ni	62.1	47.6	43.2	46.0	46.1	55.8	53.9	50.4	60.7	60.0		

Continued Table 2

Sample	QTZ11	QTZ12	QTZ13	QTZ14	QTZ15	QTZ16	QTZ17	QTZ18	QTZ19	QTZ20
Cu	65.2	68.4	40.3	36.8	44.5	46.4	3.24	35.8	56.4	85.5
Zn	130	95.9	90.6	97.6	119	120	132	114	171	153
Ga	29.2	27.7	29.1	25.3	28.2	29.0	29.2	28.9	29.8	30.6
Rb	123	163	193	150	176	174	172	155	192	188
Sr	74.0	93.2	28.0	54.2	57.1	43.2	60.6	91.2	46.4	45.3
Mo	0.17	0.09	0.18	0.15	0.09	0.05	0.05	0.05	0.05	0.05
Cd	0.08	0.05	0.31	0.05	0.07	0.18	0.05	0.05	0.05	0.09
In	0.08	0.08	0.09	0.08	0.08	0.09	0.09	0.08	0.08	0.09
Cs	4.43	6.04	7.31	5.66	6.62	6.54	6.45	5.75	7.91	8.07
Ba	1355	1759	1930	1560	1406	1594	1455	950	1273	970
Tl	0.48	0.66	0.82	0.62	0.72	0.71	0.68	0.62	0.74	0.73
Pb	16.1	13.5	36.7	5.07	11.1	5.77	4.09	7.29	8.61	11.2
Bi	0.50	1.92	0.59	0.09	0.41	0.24	0.17	0.13	0.20	0.62
Th	21.0	22.9	23.1	21.2	20.8	23.7	23.8	19.7	16.2	16.8
U	2.91	3.68	3.36	2.48	2.26	2.29	2.17	2.27	1.97	1.98
Nb	13.8	14.7	15.3	12.9	14.1	14.1	14.8	13.9	13.8	14.0
Ta	1.11	1.22	1.27	1.07	1.16	1.17	1.24	1.12	1.11	1.12
Zr	93.4	106	142	95.4	98.2	94.3	108	96.8	87.8	88.1
Hf	3.02	3.45	4.00	3.29	3.21	3.20	3.70	3.24	3.04	3.00
Sn	3.84	4.13	4.45	3.64	3.99	4.10	4.10	3.91	3.73	3.76
Sb	0.71	0.43	0.48	0.52	0.94	0.43	0.87	0.29	0.70	0.71
Ti	4101	4363	4736	3904	4260	4276	4517	4344	4744	4821
W	2.43	2.36	2.58	2.20	2.44	2.47	2.60	2.25	2.23	2.02
As	0.62	0.44	1.94	0.72	10.6	1.60	1.12	0.60	0.62	0.64
V	80.6	117	110	97.7	100	99.1	99.4	108	130	133
La	41.7	21.3	64.0	28.2	44.1	58.8	52.1	45.5	51.0	46.4
Ce	93.0	98.1	94.8	52.6	97.8	106	113	102	80.6	100
Pr	9.25	5.31	13.0	6.63	9.87	13.4	11.6	10.0	12.1	10.3
Nd	32.8	16.9	45.8	26.7	34.9	49.6	41.6	35.2	50.9	37.2
Sm	6.32	4.12	7.79	4.73	6.94	9.39	8.34	6.94	9.11	6.80
Eu	1.03	0.75	1.33	0.76	1.25	1.79	1.62	1.26	1.79	1.26
Gd	4.99	3.56	6.38	4.08	5.96	8.05	6.93	5.86	7.29	5.58
Tb	0.87	0.66	1.11	0.78	1.04	1.38	1.20	1.04	1.25	1.00
Dy	4.08	3.57	5.17	4.21	5.00	6.52	5.82	5.02	5.66	4.65
Ho	0.82	0.74	1.03	0.90	0.98	1.27	1.14	1.01	1.09	0.93
Er	2.40	2.28	2.96	2.55	2.85	3.53	3.19	2.87	3.01	2.66
Tm	0.34	0.35	0.42	0.37	0.39	0.50	0.44	0.40	0.43	0.39
Yb	2.31	2.43	2.77	2.43	2.64	3.31	2.90	2.72	2.90	2.46
Lu	0.34	0.36	0.40	0.36	0.40	0.48	0.43	0.40	0.44	0.37
Sc	18.0	18.2	18.8	16.4	18.4	18.8	19.5	18.9	19.5	20.4
Y	23.7	18.3	28.6	24.8	27.8	34.3	31.6	27.8	28.6	27.1

sedimentary rocks in this study with the characteristic age spectra of the Yangtze and Cathaysia blocks (Fig. 10) can effectively identify the provenances of these sedimentary rocks. The detrital zircon age data in this study possess three major age populations as: 900–1200 Ma, 1400–1800 Ma and 2400–2700 Ma for the Tianmashan Formation (Fig. 10). About 50% of the zircons with ages ranging from 800–1200 Ma are dominant. The previous studies have shown that the Cathaysia Block is characterized by the extensive detrital zircons of Grenvillian (1.0–1.3 Ga) and Neoarchean (2.4–2.7 Ga) ages (Wang et al., 2008; Yu et al., 2008, 2010). In contrast, The Yangtze Block contain a large number of Neoproterozoic (700–860 Ma) tectonic thermal event, which is very intense around the Yangtze Block, but weak in the Cathaysia Block. Although some ~1000 Ma detrital zircons have been found from the Kunyang Group in the southwestern Yangtze Block (Greentree et al., 2006), they are much far from the study area, and not dominant in the southwestern Yangtze Block. In comparison with Wuyi and Yunkai areas in the Cathaysia Block, the Tianmashan Formation displays similar age peaks at 1000 Ma, 1700 Ma and 2500 Ma, sources of these ages are missing in the Yangtze Block.

The frequency spectra of zircon ages are also consistent with the Bianxi Formation, Huangyi Formation in the northern margin of the Cathaysia Block, but different from the detrital zircon age spectra of the Yangtze Block (Fig. 9; age peaks at 1.0 Ga, 1.85 Ga and 2.5 Ga; Zhang et al 2016). In addition, unimodal cross-bedding is also obviously observable in fine-grained sandstone rocks of the Tianmashan Formation (Fig. 3), paleocurrent directions indicate that sediment derive from the present day south-easterly direction (Fig. 9). From the above, the sedimentary rocks from the Tianmashan Formation contain a large number of 900–1200 Ma detrital zircons and less 700–860 Ma and 1900–2100 Ma detrital zircon grains, much similar to the age spectrum of the Cathaysia Block. We demonstrated that the sedimentary basin in central Hunan province area began to accept the detrital materials from the Cathaysia Block in late Ordovician. In other words, the provenances of sedimentary basin in central Hunan province area significantly changed from the lower Ordovician to upper Ordovician. This conclusion indicates that (1) the Ordovician sedimentary basin in central Hunan area is near the border of the Yangtze and Cathaysia blocks, because it received the

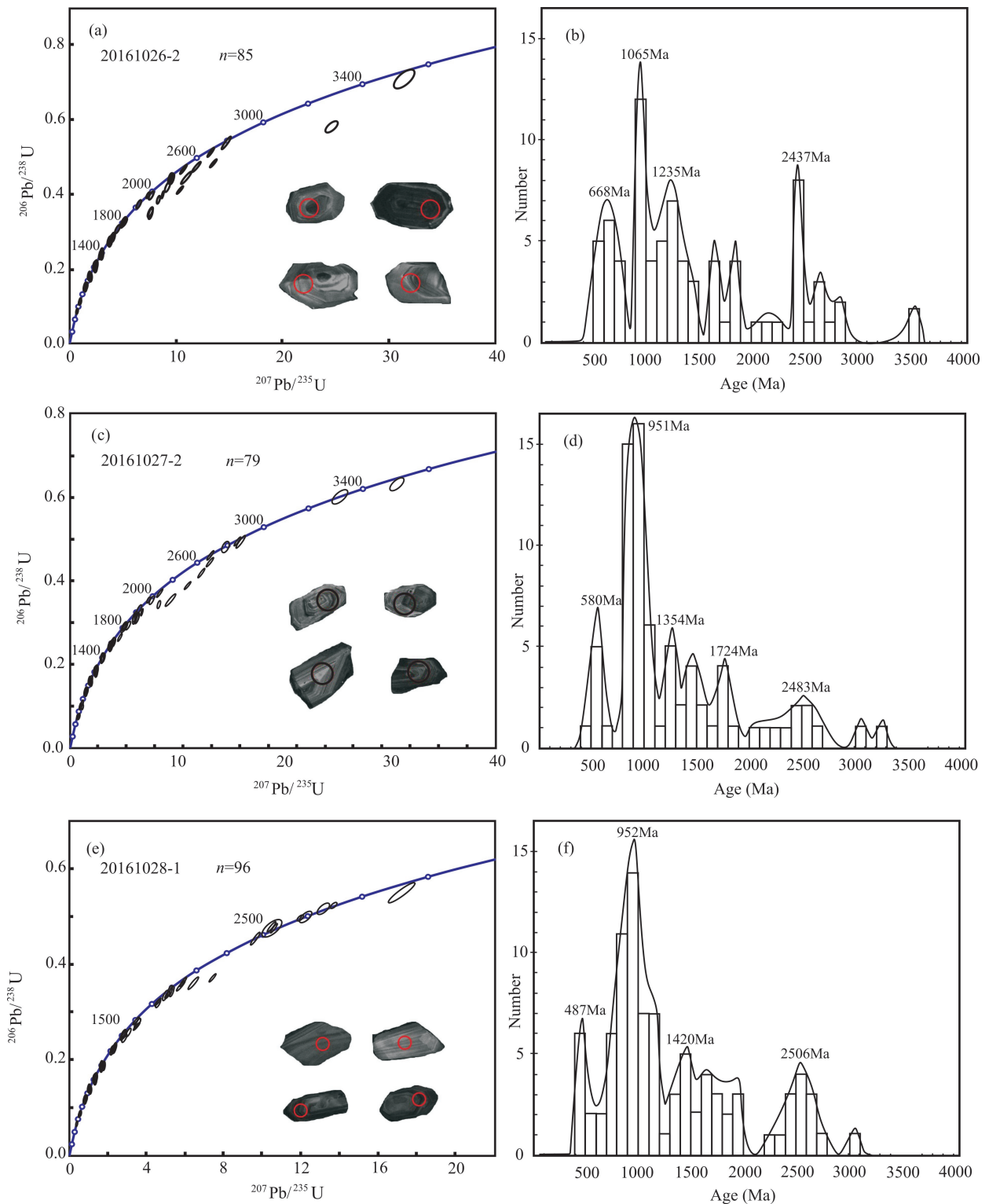


Fig. 5. U-Pb concordia plots, CL images and probability density for detrital zircons from sedimentary samples of Tianmashan Fm. in Hunan province. The red indicate the U-Pb spots. $^{206}\text{Pb}/^{238}\text{U}$ ages are used for zircons < 1.0 Ga and $^{207}\text{Pb}/^{206}\text{Pb}$ ages are used for all zircon grains > 1.0 Ga.

clastic materials from both blocks; and (2) The orogenic event occurred in late Ordovician, which caused the sinking of the basins and the final convergence between Yangtze and Cathaysia blocks in the SCB (Chen et al.,

2010; Wang et al., 2010b, 2011b), the basin setting also changed from passive continental margin basin to foreland basin, so that the basin can receive the detritus from the Cathaysia Block.

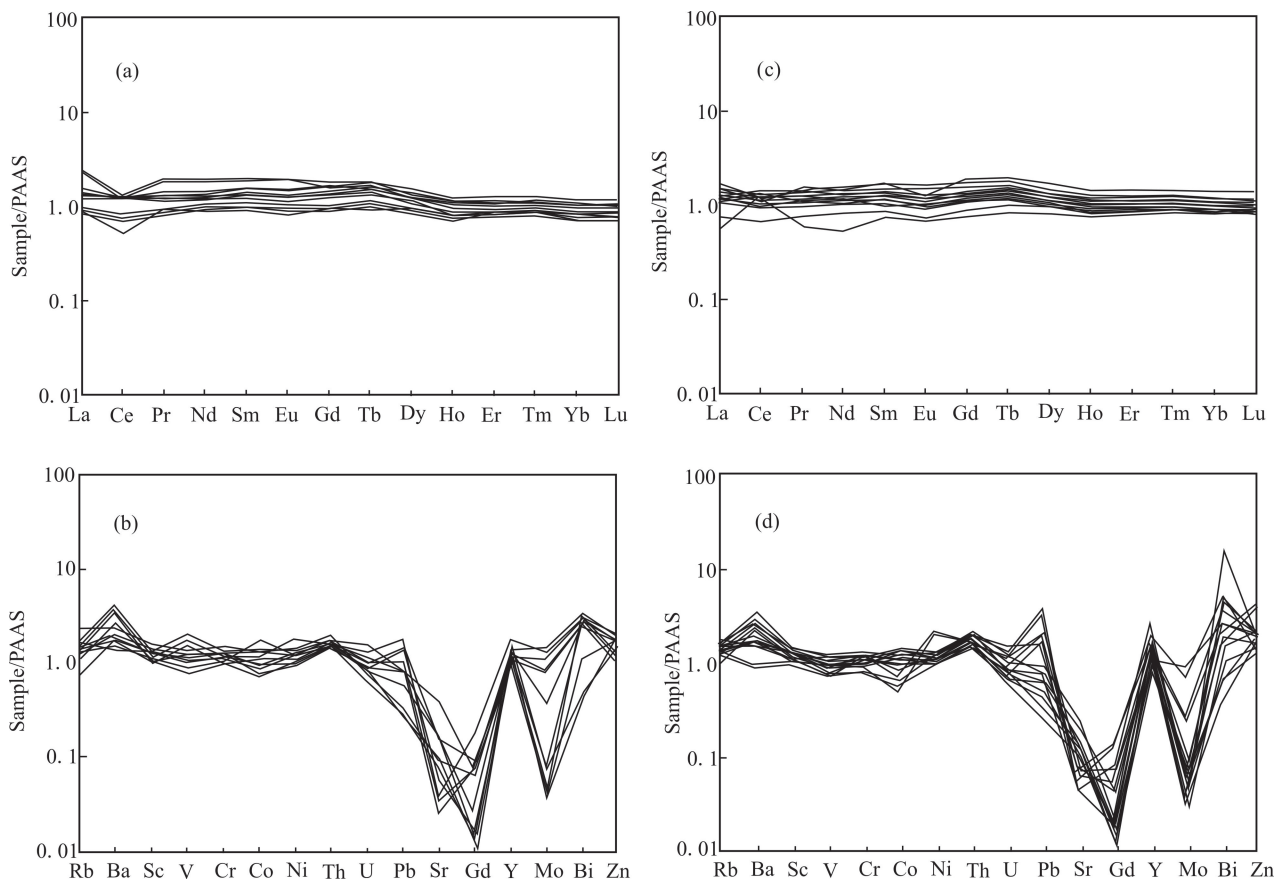


Fig. 6. PAAS (Post-Archean Australia shales) normalized REE and trace elements patterns for the sedimentary samples of Hunan Province. The normalization values are cited from Taylor and McLennan (1995).

6.2 Tectonic implications

6.2.1 Late Ordovician orogeny in the South China Block

Caledonian orogeny is the most important tectonic movement during early Paleozoic in SCB (Xu et al., 1996; Bai et al., 2007; Chen et al., 2012). This tectonic event was firstly termed as “the Kwangian movement” by Ting (1929). Chen et al. (2010) re-employed the “Kwangian movement” to explain the early Paleozoic tectonic event in the SCB. The Caledonian orogeny resulted in an unconformity between pre-Devonian and Devonian strata in the SCB (BGMRGZAR, 1985; BGMRGZ, 1988). The unconformity surface overlaps gradually younger strata from south to north across the southeastern Yangtze Block and Cathaysia Block (Bai et al., 2007; Chen et al., 2012), imply that the impact of this orogeny spread throughout SCB during early Paleozoic. The different sediment sources between the Baishuixi Formation, Qiaotingzi Formation and Tianmashan Formation imply that paleo-South China ocean between the Yangtze Block and Cathaysia blocks did not closure until the Caledonian period, leading to final amalgamation of the Yangtze and Cathaysia blocks (Wang et al., 1986; Shui, 1987; Xu et al., 1996; Ma et al., 2004; Chen et al., 2006). The following geological evidence further consistent with a subduction

tectonic regime during early Paleozoic period. (1) Abundant magmatic rocks related to subduction and collision in the northwestern Cathaysia Block in early Paleozoic time (Wang et al., 2004; Xu et al., 2009; Xi et al., 2019). (2) The differences in spatial distribution characteristics between southern Yangtze Block and northern Cathaysia Block indicate that the two blocks are not directly connected during late Ordovician (Fig. 10). With the end of subduction, the basin evolving from a shallow water predominated depositional environment in the early Ordovician, to a deep water setting in the late Ordovician (Fig. 12). In addition, the youngest detrital zircon in Tianmashan Formation yielded the maximum depositional age of around 453 Ma, suggest that the Caledonian orogeny in SCB began no later than 453 Ma.

6.2.2 Affinity of South China Block with other major continents

The comparison of age spectra with other blocks or domains can effectively provide a better comprehending on the evolution process and affinity of SCB in relation to global continental accretion events (Rino et al., 2004; Condé et al., 2009). The spectra of detrital zircons from Cathaysia and Greater as well as Lesser Himalaya record common age peaks at ca. 950 Ma (Fig. 11), implying their close affinity during the amalgamation of Rodinia

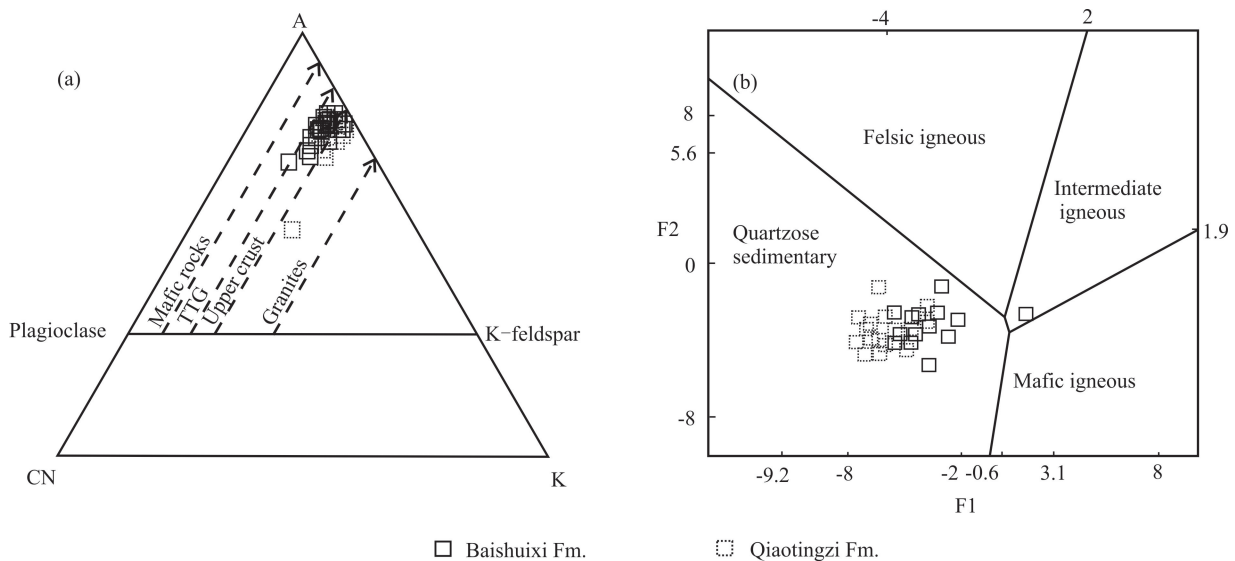


Fig. 7. Source rock discrimination diagrams for the Baishuixi and Qiaotingzi Fm. sediments. (a) A–CN–K triangle plot after Nesbitt et al. (1982); (b) F1 vs. F2 discrimination diagrams (after Roser et al., 1988).

$$\begin{aligned} \text{F1} &= -1.773\text{TiO}_2 + 0.607\text{Al}_2\text{O}_3 + 0.76\text{Fe}_2\text{O}_3\text{T} - 1.5\text{MgO} + 0.616\text{CaO} + 0.509\text{Na}_2\text{O} - 1.224\text{K}_2\text{O} - 9.09; \\ \text{F2} &= 0.445\text{TiO}_2 + 0.07\text{Al}_2\text{O}_3 - 0.25\text{Fe}_2\text{O}_3\text{T} - 1.142\text{MgO} + 0.438\text{CaO} + 1.475\text{Na}_2\text{O} + 1.426\text{K}_2\text{O} - 6.861 \end{aligned}$$

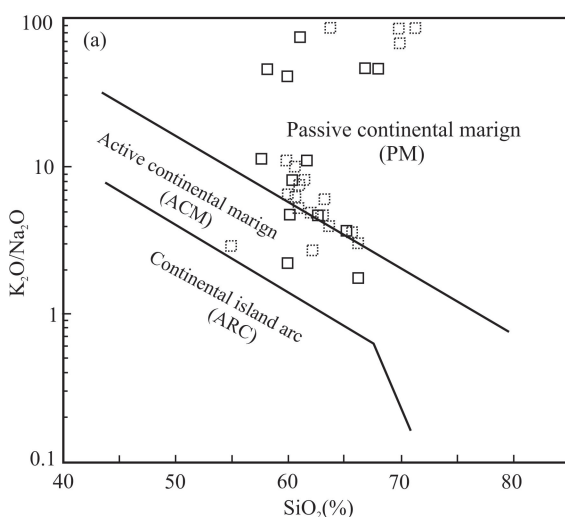


Fig. 8. Tectonic discrimination plots for the Baishuixi and Qiaotingzi Fm. sediments.
(a) $\text{K}_2\text{O}/\text{Na}_2\text{O}$ – SiO_2 (after Roser et al., 1986) and La–Th–Sc ternary diagrams (after Bhatia and Crook., 1986).

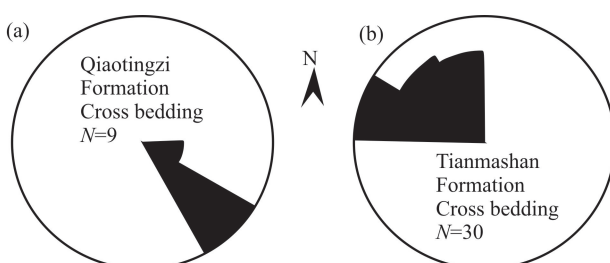


Fig. 9. Paleocurrent directions are measured from the cross-bedded sandstone of the (a) Qiaotingzi Formation and (b) Tianmashan Formation.

supercontinent. However, this event is later (850–900 Ma) in East India–East Antarctica, and older (1100–1200 Ma)

in Western Australia, confirming the diachronic nature with the assembly of Rodinia (Li et al., 2008b). Paleoproterozoic and Mesoproterozoic tectonic and magmatic imprints are relatively weak in the Nanling–Yunkai area of Cathaysia, Greater and Lesser Himalaya and Southeastern Australia, suggesting a remote relationship among these blocks and the Columbia supercontinent (Fig. 11). The late-Archean to early-Paleoproterozoic crust growth events mainly occurred during 2600–2800 Ma in Western Australia but took place at around 2400–2600 Ma in the Central Yangtze, Cathaysia, East India–East Antarctica, Southeastern Australia and Greater and Lesser Himalaya. In conclusion, the Ordovician age distributions from Hunan areas display major age peak at 900–850 Ma and minor peaks at 1600–1900 and 2400–2600 Ma. These are similar to those in

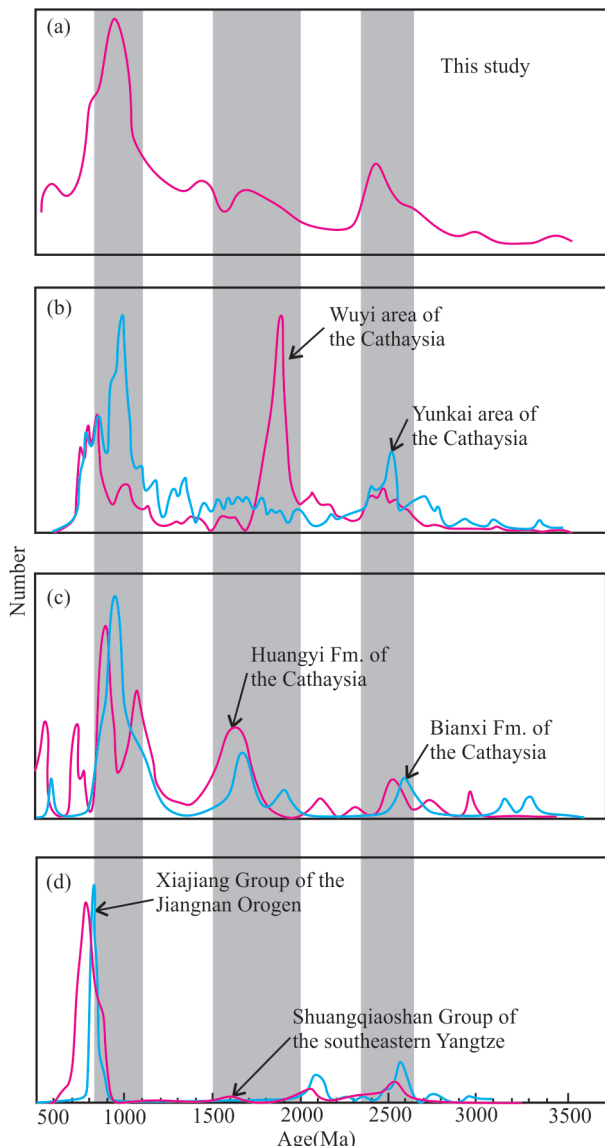


Fig. 10. Comparison of probability plots of age distributions for zircon ages from Precambrian to Ordovician sedimentary or magmatic rocks from various parts of South China Block. (a) This study; (b) Wuyi and Yunkai area of the Cathaysia (Wang et al., 2013a); (c) Huangyi and Bianxi Fm. of the Cathaysia (Zhang et al., 2016); (d) Xiajiang and Shuangqiaoshan groups (Sun et al., 2018; Yang et al., 2018).

East India–East Antarctica, Greater and Lesser Himalaya and Cathaysia but different from Southeastern and Western Australia. Thus we suggest that the SCB has a close affinity with the East India–East Antarctica, Greater and Lesser Himalaya and Cathaysia blocks (Yang et al., 2004) during the late Ordovician and Silurian.

7 Conclusions

The petrographic and geochemical data indicate that the depositional environment of the Baishuixi and Qiaotingzi Formations is the passive continental margin but the Tianmashan Formation deposited in a foreland basin during Ordovician periods.

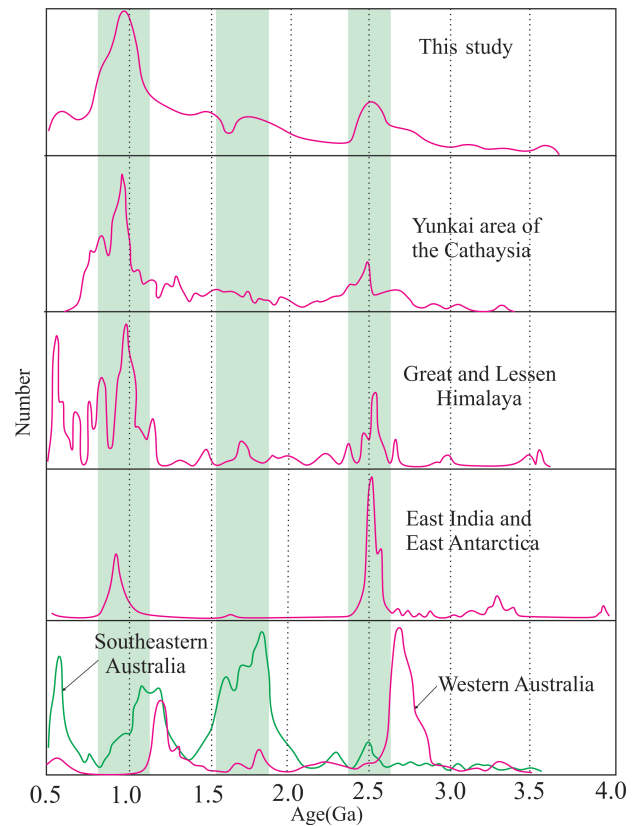


Fig. 11. Comparison of age distribution in this study with detrital zircon ages in other major global blocks.

(a) This study; (b) Yunkai area of the Cathaysia Block (Wang et al., 2013a); (c) Greater and Lesser Himalaya (Gehrels et al., 2003); (d) East India and East Antarctica (Yu et al., 2008); (e) Western Australia and Southeastern Australia (Griffin et al., 2004; Veevers et al., 2005; Condie et al., 2009).

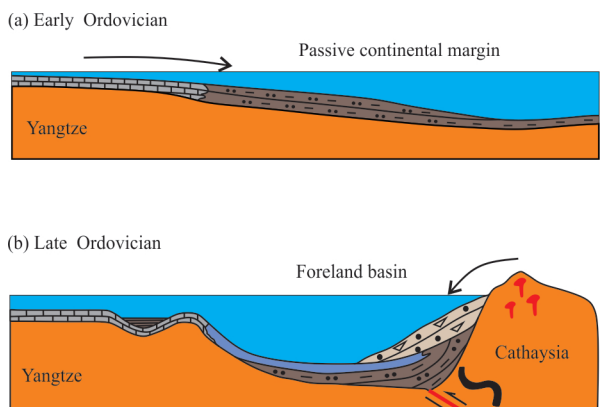


Fig. 12. Schematic model for the Ordovician evolution of the South China Block.

The Tianmashan Formation sedimentary rocks contain abundant Grenville-aged detrital zircons, consistent with the characteristic age peak of Cathaysia Block, implying the affinity with the Cathaysia Block.

The change of provenances between the lower and upper Ordovician strata suggests that a tectonic movement occurred during late Ordovician period, which is the

response of the Caledonian movement in the SCB.

Acknowledgements

This research was financially supported by the China Geological Survey (Nos. DD20190370, 121201111120117 and 121201102000150012–32). We are grateful to Wang Yan of the Key Laboratory of Mineralization and Resource Evaluation, Chinese Academy of Geological Sciences and He Rong of Institute of Geology, Chinese Academy of Geological Sciences as well as other workers for their assistance.

Manuscript received Apr. 7, 2019
accepted Sept. 15, 2020
associate EIC: FEI Hongcai
edited by FANG Xiang

References

- Bai, D.Y., Zhou, L., Wang, X.H., Zhang, Z.Y., and Ma, T.Q., 2007. Geochemistry of Nanhuan–Cambrian sandstones in southeastern Hunan, and its constraints on Neoproterozoic–Early Paleozoic tectonic setting of South China. *Acta Geologica Sinica*, 81(6): 755–771 (in Chinese with English Abstract).
- Belousova, E.A., Griffin, W.L., O'Reilly, S.Y., and Fisher, N., 2002. Igneous zircon: trace element composition as an indicator of source rock type. *Contributions to Mineralogy and Petrology*, 143: 602–622.
- BGMRGP (Bureau of Geology and Mineral Resources of Guangdong Province), 1988. Regional Geology of the Guangdong Province. Beijing: Geological Publishing House, 1–941 (in Chinese with English abstract).
- BGMRGZAR (Bureau of Geology and Mineral Resources of Guangxi Zhuang Autonomous Region), 1985. Regional Geology of the Guangxi Zhuang Autonomous Region. Geological Publishing House, Beijing, 1–853 (in Chinese with English abstract).
- BGMRHN (Bureau of Geology and Mineral Resources of Hunan Province), 1988. Regional Geology of the Hunan Province. Beijing: Geological Publishing House. 663 (in Chinese with English abstract).
- Bhatia, M.R., 1983. Plate tectonics and geochemical composition of sandstones. *Journal of Geology*, 91: 611–627.
- Bhatia, M.R., and Crook, K.A.W., 1986. Trace element characteristics of graywackes and tectonic setting discrimination of sedimentary basins. *Contrib. Miner. Petrol.* 92: 181–193.
- Chen, H.D., Hou, M.C., Xu, X.S., and Tian, J.C., 2006. Tectonic evolution and sequence stratigraphic framework in South China during Caledonian. *Journal of Chengdu University of Technology*, 33 (1): 1–8.
- Chen, L., Wang, Z.Q., Yan, Z., Gong, J.H., and Ma, S.X., 2018. Zircon and cassiterite U–Pb ages, petrogeochemistry and metallogenesis of Sn deposits in the Sibao area, northern Guangxi: constraints on the neoproterozoic granitic magmatism and related Sn mineralization in the western Jiangnan Orogen, South China. *Mineralogy and Petrology*, 112: 437–463.
- Chen, X., Rong, J.Y., Mitchell, C.E., Happer, D.A.T., Fan, J.X., Zhan, R.B., Zhang, Y.D., Li, R.Y., and Wang, Y., 2000. Late Ordovician to earliest Silurian graptolite and brachiopod zonation from Yangtze Region, South China with a global correlation. *Geological Magazine*, 137 (6): 623–650.
- Chen, X., Fan, J.X., Zhan, R.B., Mitchell, C.E., Harper, D.A.T., Melchin, M.J., Peng, P.A., Finney, S.C., and Wang, X.F., 2006. A final report on the Global Stratotype Section and Point(GSSP) for the Hirnantian stage (upper Ordovician). *Journal of Stratigraphy*, 30(04): 289–305+393–394.
- Chen, X., Zhang, Y.D., Fan, J.X., Cheng, J.F., and Li, Q.J., 2010. Ordovician graptolite-bearing strata in southern Jiangxi with a special reference to the Kwangsi Orogeny. *Science in China (Earth Sciences)*, 53(1): 1602–1610.
- Chen, X., Zhang, Y.D., Fan, J.X., Tang, L., and Sun, H.Q., 2012. Onset of the Kwangsi Orogeny as evidenced by biofacies and lithofacies. *Science China: Earth Sciences*, 55: 1592–1600.
- Condie, K.C., Belousova, E., Griffin, W.L., and Sircombe, K.N., 2009. Granitoid events in space and time: constraints from igneous and detrital zircon age spectra. *Gondwana Research*, 15(3–4): 228–242.
- Corfu, F., Hanchar, J.M., Hoskin, P.W.O., and Kinny, P., 2003. Altas of zircon textures. *Reviews in Mineralogy and Geochemistry*, 53: 469–500.
- Fedo, C.M., Sircombe, K.N., and Rainbird, R.H., 2003. Detrital zircon analysis of the sedimentary record. *Reviews in Mineralogy and Geochemistry*, 53: 277–303.
- Gao, S., Lin, W.L., and Qiu, Y.M., 1999. Contrasting geochemical and Sm–Nd isotopic compositions of Archaean metasediments from the Kongling high-grade terrain of the Yangtze craton: evidence for cratonic evolution and redistribution of REE during crustal anatexis. *Geochimica et Cosmochimica Acta*, 13 (14): 2071–2088.
- Gehrels, G.E., Yin, A., and Wang, X., 2003. Detrital zircon geochronology of the northeastern Tibetan plateau. *Geological Society of America Bulletin*, 115: 881–896.
- Geng, Y.S., Kuang, H.W., Liu, Y.Q., and Du, L.L., 2017. Subdivision and correlation of the Mesoproterozoic stratigraphy in the western and northern margins of Yangtze block. *Acta Geologica Sinica*, 91(10): 2151–2174 (in Chinese with English abstract).
- Greentree, M.R., Li, Z.X., Li, X.H., and Wu, H.C., 2006. Late Mesoproterozoic to earliest Neoproterozoic basin record of the Sibao orogenesis in western South China and relationship to the assembly of Rodinia. *Precambrian Research*, 151: 79–100.
- Greentree, M.R., and Li, Z.X., 2008. The oldest known rocks in south-western China: SHRIMP U–Pb magmatic crystallization age and detrital provenance analysis of the Paleoproterozoic Dahongshan Group. *Journal of Asian Earth Sciences*, 33, 289–302.
- Griffin, W.L., Belousova, E.A., Shee, S.R., Pearson, N.J., and O'Reilly, S.Y., 2004. Archaean crustal evolution in the northern Yilgarn Craton: U–Pb and Hf-isotope evidence from detrital zircons. *Precambrian Research*, 131: 231–282.
- Guo, F.S., Shi, G., Yang, Q.K., Zhang, W.L., Xie, C.F., Zhou, W.P., and Zhang, J.W., 2018. Timing of metamorphism and provenance of the metamorphic basement of the Xiangshan uranium orefield, Jiangxi Province, China. *Acta Geologica Sinica (English Edition)*, 92(1): 34–55.
- Jiang, X.F., Peng, S.B., Timothy M. Kusky, Wang, L., and Deng, H., 2018. Petrogenesis and Geotectonic Significance of Early–Neoproterozoic Olivine–Gabbro within the Yangtze Craton: Constraints from the Mineral Composition, U–Pb Age and Hf Isotopes of Zircons. *Journal of Earth Science*, 29: 93–102.
- Li, L.M., Sun, M., Wang, Y.J., Xing, G.F., Zhao, G.C., Cai, K.D., and Zhang, Y.Z., 2011a. Geochronological and geochemical study of Palaeoproterozoic gneissic granites and clinopyroxenite xenoliths from NW Fujian, SE China: implications for the crustal evolution of the Cathaysia Block. *Journal of Asian Earth Sciences*, 41: 204–212.
- Li, X.H., Li, W.X., Li, Z.X., Lo, C.H., Wang, J., Ye, M.F., and Yang, Y.H., 2009. Amalgamation between the Yangtze and Cathaysia blocks in South China: Constraints from SHRIMP U–Pb zircon ages, geochemistry and Nd–Hf isotopes of the Shuangxiu volcanic rocks. *Precambrian Research*, 174: 117–128.
- Li, Z.X., Li, X.H., Zhou, H.W., and Kinny, P.D., 2002. Grenvillian continental collision in south China: New SHRIMP U–Pb zircon results and implications for the configuration of Rodinia. *Geology*, 2: 163–166.
- Li, Z.X., Li, X.H., Kinny, P.D., Wang, J., Zhang, S., and Zhou, H., 2003. Geochronology of Neoproterozoic syn-rift magmatism in the Yangtze craton, South China and correlations with other continents: evidence for a mantle superplume that broke up Rodinia. *Precambrian Research*,

- 122: 85–109.
- Li, Z.X., Wartho, J.A., Occhipinti, S., Zhang, C.L., Li, X.H., Wang, J., and Bao, C., 2007. Early history of the eastern Sibao Orogen (South China) during the assembly of Rodinia: new mica $^{40}\text{Ar}/^{39}\text{Ar}$ dating and SHRIMP U–Pb detrital zircon provenance constraints. *Precambrian Research*, 159(1): 79–94.
- Li, Z.X., Bogdanova, S.V., Collins, A.S., Davidson, A., De Waele, B., Ernst, R.E., Fitzsimons, I.C.W., Fuck, R.A., Gladkochub, D.P., Jacobs, J., Karlstrom, K.E., Lu, S., Natapov, L.M., Pease, V., Pisarevsky, S.A., Thrane, K., and Vernikovsky, V., 2008b. Assembly, configuration, and break-up history of Rodinia: a synthesis. *Precambrian Research*, 160: 179–210.
- Li, Z.X., Li, X.H., Wartho, J.A., Clark, C., Li, W.X., Zhang, C.L., and Bao, C.M., 2010. Magmatic and metamorphic events during the Early Paleozoic Wuyi–Yunkai Orogeny, southeastern South China: new age constraints and P–T conditions. *GSA Bulletin*, 122(5–6): 772–793.
- Liu, Y., Gao, S., Hu, Z., Gao, C., Zong, K., and Wang, D., 2010. Continental and oceanic crust recycling-induced melt peridotite interactions in the Trans–North China Orogen: U–Pb dating Hf isotopes and trace elements in zircons of mantle xenoliths. *Journal of Petrology*, 51: 537–571.
- Ludwig, K.R. ISOPLOT 3.00: A Geochronological Toolkit for Microsoft Excel Berkeley. 1–10.
- Luo, W., He, Y.B., Jiang, J.J., and You, G.Q., 2012. An analysis of Ordovician rock association and sedimentary environment in southern Hunan Province. *Geological Bulletin of China*, 31 (7): 1105–1114 (in Chinese with English Abstract).
- Ma, L., Chen, H.J., Gan, K.W., Xu, X.S., Wu, G.Y., Ye, Z., Liang, X., Wu, S.H., Qiu, Y.Y., Zhang, P.L., and Ge, P.P., 2004. Geotectonics and petroleum geology of marine sedimentary rocks in southern China. Beijing: Geological Publishing House, 1–867.
- McLennan, S.M., Hemming, S.R., Taylor, S.R., and Eriksson, K.A., 1995. Early Proterozoic crustal evolution: geochemical and Nd–Pb isotopic evidence from metasedimentary rocks, southwestern North America. *Geochimica et Cosmochimica Acta*, 59: 1153–1177.
- Nesbitt, H.W., and Young, G.M., 1982. Early Proterozoic climates and plate motions inferred from major element chemistry of lutites. *Nature*, 299: 715–717.
- Qiu, Y.M., Gao, S., McNaughton, N.J., Groves, D.I., and Ling, W.L., 2000. First evidence of >3.2 Ga continental crust in the Yangtze craton of South China and its implications for Archean crustal evolution and Phanerozoic tectonics. *Geology*, 28(1): 11–14.
- Ren, J.S., 1991. On the geotectonics of southern China. *Acta Geologica Sinica* (English Edition), 65(2): 111–136.
- Rino, S., Komiya, T., Windley, B.F., Katayama, I., Motoki, A., and Hirata, T., 2004. Major episodic increases of continental crustal growth determined from zircon ages of river sands: implications for mantle overturns in the early Precambrian. *Physics of the Earth and Planetary Interiors*, 146: 369–394.
- Roser, B.P., and Korsch, R.J., 1986. Determination of Tectonic Setting of Sandstone–mudstone Suites Using SiO_2 Content and $\text{K}_2\text{O}/\text{Na}_2\text{O}$ Ratio. *The Journal of Geology*, 94(5): 635–650.
- Shu, L.S., and Charvet, J., 1996. Kinematics and geochronology of the Proterozoic Dongxiang–Shebian ductile shear zone (Jiangnan region, South China). *Tectonophysics*, 267(14): 291–302.
- Shu, L.S., and Zhou, X.M., 2002. Late Mesozoic Tectonism of Southeast China. *Geological Review*, 48(3): 249–260 (in Chinese with English Abstract).
- Shu, L.S., 2006. Predevonian tectonic evolution of South China: from Cathaysian Block to Caledonian period folded orogenic belt. *Geological Journal of China Universities*, 12(4): 418–431 (in Chinese with English Abstract).
- Shui, T., 1987. Tectonic framework of the southeastern China continental basement. *Scientia Sinica* B30, 414–421 (in Chinese with English Abstract).
- Ting, V.K., 1929. The orogenic movements in China (Presidential Address of the 6th Annual Meeting). *Bulletin of Geological Society of China*, 8: 151–170.
- Wan, Y.S., Liu, D.Y., Xu, M.H., Zhuang, J., Song, B., Shi, Y., and Du, L., 2007. SHRIMP U–Pb zircon geochronology and geochemistry of metavolcanic and metasedimentary rocks in Northwestern Fujian, Cathaysia Block, China: tectonic implications and the need to redefine lithostratigraphic units. *Gondwana Research*, 12: 166–183.
- Wang, D., Wang, X.L., Zhou, J.C., and Shu, L.S., 2013a. Unraveling the Precambrian crustal evolution by Neoproterozoic conglomerates, Jiangnan orogen: U–Pb and Hf isotopes of detrital zircons. *Precambrian Research*, 233: 223–236.
- Wang, D.Z., 2004. The study of granitic rocks in South China: looking back and forward. *Geological Journal of China Universities*, (03): 305–314 (in Chinese with English Abstract).
- Wang, H.Z., Yang, W.R., and Liu, B.P., 1986. Tectonic history of the ancient continental margins of South China. Wuhan: Wuhan Geological Institute Publishing House (in Chinese).
- Wang, J., Liu, B.J., and Pan, G.T., 2001. Neoproterozoic rifting history of South China significance to Rodinia breakup. *Jmineral Petrol*, 03: 135–145.
- Wang, L.J., Yu, J.H., O'Reilly, S.Y., Griffin, W.L., Sun, T., Wei, Z.Y., Jiang, S.Y., and Shu, L.S., 2008. Grenvillian orogeny in the Southern Cathaysia Block: constraints from U–Pb ages and Lu–Hf isotopes in zircon from metamorphic basement. *Chinese Science Bulletin*, 53: 3037–3050.
- Wang, Q., Wymore, D.A., Li, Z.X., Bao, Z.W., Zhao, Z.H., and Wang, Y.X., 2010b. Petrology, geochronology and geochemistry of ca. 780 Ma A-type granites in South China: petrogenesis and implications for crustal growth during the breakup of the supercontinent Rodinia. *Precambrian Research*, 178: 185–208.
- Wang, X.L., Zhou, J.C., Griffin, W.L., Wang, R.C., Qiu, J.S., O'Reilly, S.Y., Xu, X.S., Liu, X.M., and Zhang, G.L., 2007. Detrital zircon geochronology of Precambrian basement sequences in the Jiangnan orogenic belt: Dating the assembly of the Yangtze and Cathaysia Blocks. *Precambrian Research*, 159: 117–131.
- Wang, X.L., Shu, L.S., Xing, G.F., Zhou, J.C., Tang, M., Shu, X.J., Qi, L., and Hu, Y.H., 2012. Post-orogenic extension in the eastern part of the Jiangnan orogen: evidence from ca 800–760 Ma volcanic rocks. *Precambrian Research*, 222–223: 404–423.
- Wang, Y.J., Zhang, A.M., Fan, W.M., Zhao, G.C., Zhang, G.W., Zhang, Y.Z., Zhang, F.F., and Li, S.Z., 2011. Kwangshian crustal anatexis within the eastern South China Block: geochemical, zircon U–Pb geochronological and Hf isotopic fingerprints from the gneissic granites of Wugong and Wuyi–Yunkai Domains. *Lithos*, 127: 239–260.
- Wu, F.J., and Zhang, F.R., 2003. Features and genesis of Caledonian granites in the Wugongshan in the eastern segment of the northern margin of South China plate. *Geology in China*, 2003, 30(2): 166–172 (in Chinese with English Abstract).
- Xi, W.W., and Chen, S.Z., 2019. Identification of Caledonian granites in the Zhenghe area, Fujian province and its tectonic significance. *Acta Geologica Sinica*, 93(4): 804–815 (in Chinese with English Abstract).
- Xiang, H., Zhang, L., Zhou, H., Zhong, Z., Zeng, W., Liu, R., and Jin, S., 2008. U–Pb zircon geochronology and Hf isotope study of metamorphosed basic–ultrabasic rocks from metamorphic basement in southwestern Zhejiang: the response of the Cathaysia Block to Indosinian orogenic event. *Science in China (Series D: Earth Sciences)*, 51: 788–800.
- Xu, X.B., Zhang, Y.Q., Shu, L.S., Jia, D., Wang, R.R., and Xu, H.Z., 2009. Zircon La–ICPMS U–Pb Dating of the Weipu Granitic Pluton in Southwest Fujian and the Changpu Migmatite in South Jiangxi: Constraints to the Timing of Caledonian Movement in Wuyi Mountains. *Geological Review*, 55(2): 277–285 (in Chinese with English Abstract).
- Xu, X.S., Xu, Q., and Pan, G.T., 1996. The continental evolution of southern China and its global comparison. Beijing: Geological Publishing House, 10–12 (in Chinese with English Abstract).
- Xu, Y.J., Du, Y.S., Cawood, P.A., Zhu, Y.H., Li, W.C., and Yu, W.C., 2012. Detrital zircon provenance of upper Ordovician

- and Silurian strata in the northeastern Yangtze block: Response to orogenesis in South China. *Sedimentary Geology*, 267: 63–72.
- Yang, M.G., Zhu, P.J., Xiong, Q.H., and Mao, S.P., 2012. Framework and evolution of the Neoproterozoic–early Paleozoic South China rift system. *Acta Geologica Sinica*, 86 (9): 1367–1375 (in Chinese with English Abstract).
- Yang, Z.Y., Sun, Z.M., Yang, T.S., and Pei, J.L., 2004. A long connection (750–380 Ma) between South China and Australia: paleomagnetic constraints. *Earth and Planetary Science Letters*, 220: 423–434.
- Yao, W.H., Li, Z.X., Li, W.X., Su, L., and Yang, J.H., 2015. Detrital provenance evolution of the Ediacaran–Silurian Nanhua foreland basin, South China. *Gondwana Research*, 28 (4): 1449–1465.
- Yao, J.L., Shu, L.S., and Santosh, M., 2014. Neoproterozoic arc–trench system and breakup of the South China Craton: Constraints from N–MORB type and arc-related mafic rocks, and anorogenic granite in the Jiangnan orogenic belt. *Precambrian Research*, 247: 187–207.
- Yao, J.L., Shu, L.S., Santosh, M., and Li, J.Y., 2015. Neoproterozoic arc-related andesite and orogeny-related unconformity in the eastern Jiangnan orogenic belt: Constraints on the assembly of the Yangtze and Cathaysia blocks in South China. *Precambrian Research*, 262: 84–100.
- Yao, J.L., Cawood, P.A., Shu, L.S., Santosh, M., and Li, J.Y., 2016. An early Neoproterozoic accretionary prism ophiolitic mélange from the western Jiangnan orogenic belt, South China. *The Journal of Geology*, 124: 587–601.
- Yin, F.G., Xu, X.S., Wang, F., and Chen, M., 2001. The sedimentary response to the evolutionary process of Caledonian foreland Basin System in South China. *Acta Geoscientia Sinica*, 22(5): 425–428.
- Yu, J.H., O'Reilly, S.Y., Wang, L.J., Griffin, W.L., Zhang, M., Wang, R.C., Jiang, S.Y., and Shu, L.S., 2008. Where was South China in the Rodinia supercontinent? Evidence from U–Pb geochronology and Hf isotopes of detrital zircons. *Precambrian Research*, 164: 1–15.
- Yu, J.H., Wang, L.J., Griffin, W.L., O'Reilly, S.Y., Zhang, M., Li, C.Z., and Shu, L.S., 2009. A Paleoproterozoic orogeny recorded in a long-lived cratonic remnant (Wuyishan terrane), eastern Cathaysia Block, China. *Precambrian Research*, 174: 347–363.
- Yu, J.H., O'Reilly, S.Y., Wang, L.J., Griffin, W.L., Zhou, M.F., Zhang, M., and Shu, L.S., 2010. Components and episodic growth of Precambrian crust in the Cathaysia Block, south China: evidence from U–Pb ages and Hf isotopes of zircons in Neoproterozoic sediments. *Precambrian Research*, 181: 97–114.
- Yuan, Z.X., and Zhong, G.F., 1997. A new recognition on spacio-temporal characteristics of the Caledonian orogeny happened in south China.
- Zhang, X., Zeng, Z.X., Liu, W., Pan, L.L., Yang, B.Z., Liu, J.X., Wei, Y.X., He, C.C., and Li, S.F., 2016. Detrital zircon geochronology of Cambrian–Ordovician sedimentary rocks in southern Hunan–Northeast Guangxi area and its tectonic implications. *Geology in China*, 43(1): 153–173 (in Chinese with English abstract).
- Zhao, G.C., and Cawood, P.A., 1999. Tectonothermal evolution of the Mayuan assemblage in the Cathaysia Block: implications for Neoproterozoic collision-related assembly of the South China craton. *American Journal of Science*, 299: 309–339.
- Zhao, G.C., 2015. Jiangnan Orogen in South China: Developing from divergent double subduction. *Gondwana Research*, 27: 1173–1180.
- Zhao, X.F., Zhou, M.F., Li, J.W., Sun, M., Gao, J.F., Sun, W.H., and Yang, J.H., 2010. Late Paleoproterozoic to early Mesoproterozoic Dongchuan Group in Yunnan, SW China: Implications for tectonic evolution of the Yangtze Block. *Precambrian Research*, 182: 57–69.
- Zhao, Z.B., Xu, Z.Q., Ma, X.X., Liang, F.H., and Guo, P., 2018. Neoproterozoic–Early Paleozoic tectonic evolution of the South China Craton: New insights from the polyphase deformation in the southwestern Jiangnan orogen. *Acta Geologica Sinica (English Edition)*, 92(5): 1700–1727.
- Zheng, J.P., Griffin, W.L., O'Reilly, S.Y., Zhang, M., and Pearson, N., 2006. Widespread Archean basement beneath the Yangtze craton. *Geology*, 34: 417–420.
- Zheng, Y.F., Zhang, S.B., Zhao, Z.F., Wu, Y.B., Li, X.H., Li, Z.X., and Wu, F.Y., 2007. Contrasting zircon Hf and O isotopes in the two episodes of Neoproterozoic granitoids in South China: implications for growth and reworking of continental crust. *Lithos*, 96: 127–150.
- Zheng, Y.F., Wu, R.X., Wu, Y.B., Zhao, Z.F., Zhang, S.B., Yuan, H.L., and Wu, F.Y., 2008. Rift melting of juvenile arc-derived crust: Geochemical evidence from Neoproterozoic volcanic and granitic rocks in the Jiangnan orogen, South China. *Precambrian Research*, 163: 351–383.
- Zhou, J.C., Wang, X.L., and Qiu, J.S., 2009. Geochronology of Neoproterozoic mafic rocks and sandstones from northeastern Guizhou, South China: Coeval arc magmatism and sedimentation. *Precambrian Research*, 170: 27–42.
- Zhou, M.F., Yan, D.P., Kennedy, A.K., Li, Y.Q., and Ding, J., 2002. SHRIMP U–Pb zircon geochronological and geochemical evidence for Neoproterozoic arc magmatism along the western margin of the Yangtze block, South China. *Earth and Planetary Science Letters*, 196: 51–67.

About the first author



ZHANG Jibiao, male, born in 1992 in Jinan City, Shandong Province; Ph.D candidate; He is now studying at the Institute of Geology, Chinese Academy of Geological Sciences and study on structural geology. Email: thalskmno2222@163.com; phone: 13051196998.

About the corresponding author



LIU Yanxue, male, born in 1964 in Handan City, Hebei Province; doctor; graduated from China University of Geosciences, Beijing; research fellow of Institute of Geology, Chinese Academy of Geological Sciences. He is now interested in the study on sedimentary geology. Email: 425368369@qq.com; phone: 13691280579.